SIAM J. SCI. COMPUT.
Vol. 42, No. 1, pp. A504–A533

ASYMPTOTIC APPROXIMATIONS FOR THE CLOSE EVALUATION OF DOUBLE-LAYER POTENTIALS*

CAMILLE CARVALHO†, SHILPA KHATRI†, AND ARNOLD D. KIM†

Abstract. When using boundary integral equation methods to solve a boundary value problem, the evaluation of the solution near the boundary is challenging to compute because the layer potentials that represent the solution are nearly singular integrals. To address this close evaluation problem, we develop a new numerical method by applying an asymptotic analysis of these nearly singular integrals and obtaining an asymptotic approximation. We derive the asymptotic approximation for the case of the double-layer potential in two and three dimensions, representing the solution of the interior Dirichlet problem for Laplace's equation. By doing so, we obtain an asymptotic approximation given by the Dirichlet data at the boundary point nearest to the interior evaluation point plus a nonlocal correction. We present the numerical methods using this asymptotic approximation, and we demonstrate the efficiency and accuracy of these methods and the asymptotic approximation through several examples. These examples show that the numerical method based on the asymptotic approximation accurately approximates the close evaluation of the double-layer potential while requiring only modest computational resources.

Key words. asymptotic approximation, close evaluation problem, potential theory, boundary integral equations

AMS subject classifications. 41A60, 65D30, 65R20

DOI. 10.1137/18M1218698

1. Introduction.

The close evaluation problem refers to the nonuniform error produced by high-order quadrature rules used in boundary integral equation methods. High-order quadrature rules attain spectral accuracy when computing the solution, represented by layer potentials, far from the boundary but incur a very large error when computing the solution close to the boundary. This large error incurred when evaluating layer potentials close to the boundary is called the *close evaluation problem*. It is well understood that this growth in error is due to the fact that the integrand of the layer potentials becomes increasingly peaked as the point of evaluation approaches the boundary. In fact, when the distance between the evaluation point and its closest boundary point is smaller than the distance between quadrature points on the boundary for a fixed-order quadrature rule, the quadrature points do not adequately resolve the peak of the integrand and therefore produce an $O(1)$ error.

Accurate evaluations of layer potentials close to the boundary of the domain are needed for a wide range of applications, including the modeling of swimming microorganisms, droplet suspensions, and blood cells in Stokes flow [8, 17, 23, 30], and to predict accurate measurements of the electromagnetic near-field in the field of plasmonics [22] for nanoantennas [3, 26] and sensors [24, 28].

*Submitted to the journal's Methods and Algorithms for Scientific Computing section October 5, 2018; accepted for publication (in revised form) November 12, 2019; published electronically February 25, 2020.

https://doi.org/10.1137/18M1218698

Funding: This work was funded by the National Science Foundation (grant DMS-1819052). The second author was also supported by the National Science Foundation (grant PHY-1505061). The third author was also supported by the Air Force Office of Scientific Research (grants FA9550-17-1-0238 and FA9550-18-1-0519).

†Department of Applied Mathematics, University of California, Merced, Merced, CA 95343 (ccarvalho3@ucmerced.edu, skhatri3@ucmerced.edu, adkim@ucmerced.edu).

Several computational methods have been developed to address this close evaluation problem. Schwab and Wendland [29] have developed a boundary extraction method based on a Taylor series expansion of the layer potentials. Beale and Lai [10] have developed a method that first regularizes the nearly singular kernel of the layer potential and then adds corrections for both the discretization and the regularization. Beale, Ying, and Wilson [11] have extended the regularization method to three-dimensional problems. Helsing and Ojala [15] developed a method that combines a globally compensated quadrature rule and interpolation to achieve very accurate results over all regions of the domain. Barnett [9] has used surrogate local expansions with centers placed near but not on the boundary. Klöckner et al. [20] introduced Quadrature by Expansion (QBX), which uses expansions about accurate evaluation points far away from the boundary to compute accurate evaluations close to it. There have been several subsequent studies of QBX [1, 2, 13, 27, 31] that have extended its use and characterized its behavior.

Recently, the authors have applied asymptotic analysis to study the close evaluation problem. For two-dimensional problems, the authors developed a method that used matched asymptotic expansions for the kernel of the layer potential [12]. In that method, the asymptotic expansion that captures the peaked behavior of the kernel (namely, the peaked behavior of the integrand of the layer potential) can be integrated exactly, and the relatively smooth remainder is integrated numerically, resulting in a highly accurate method. For three-dimensional problems, the authors have developed a simple three-step method for computing layer potentials [18]. This method involves first rotating the spherical coordinate system used to compute the layer potential so that the boundary point at which the integrand becomes singular is aligned with the north pole. By studying the asymptotic behavior of the integral, they found that integration with respect to the azimuthal angle after the initial rotation is a natural averaging operation that regularizes the integral and allows for a high-order quadrature rule to be used for the integral with respect to the polar angle. This numerical method was shown to achieve an error that decays quadratically with the distance to the boundary provided that the underlying boundary integral equation for the density is sufficiently resolved.

In this work, we carry out an asymptotic analysis of the close evaluation of the double-layer potential for the interior Dirichlet problem for Laplace's equation in two and three dimensions. By doing so, we derive asymptotic approximations that provide valuable insight into the inherent challenges of the close evaluation problem. These asymptotic approximations are given by the Dirichlet data at the boundary point closest to the evaluation point plus a nonlocal correction. It is the nonlocal correction that makes the close evaluation problem challenging to address. The asymptotic analysis leads to an explicit expression for this nonlocal correction and suggests a natural way to accurately and efficiently compute it. We develop new, explicit numerical methods for computing the close evaluation using these asymptotic approximations. We provide several examples that demonstrate that these methods are consistent with the expected accuracy from the asymptotic analysis.

The remainder of this paper is as follows. We precisely define the close evaluation problem for the double-layer potential and state the expected leading-order asymptotic behavior of the double-layer potential in section 2. We give the derivation in two dimensions in section 3 and three dimensions in section 4. We describe the new numerical methods using the asymptotic approximations for the close evaluation of the double-layer potential in section 5. We give several examples demonstrating the accuracy of this numerical method in section 6. Section 7 gives our conclusions. The

appendices provide details of the computations used throughout this paper: Appendix A establishes additional results we have used to justify the obtained asymptotic approximations of sections 3 and 4, Appendix B gives details of how we rotate spherical integrals, and Appendix C gives a useful derivation of the spherical Laplacian.

2. Motivation and results of asymptotic analysis. Consider a simply connected, open set, denoted by $D \subset \mathbb{R}^n$ with $n = 2, 3$, with an analytic close boundary, B, and let $\bar{D} = D \cup B$. Given some smooth data $f \in C^2(B)$, we write the function $u \in C^2(D) \cap C^1(\bar{D})$ satisfying the interior Dirichlet problem,

$$\Delta u = 0 \quad \text{in } D, \tag{2.1a}$$

$$u = f \quad \text{on } B, \tag{2.1b}$$

as the double-layer potential,

$$u(x) = \frac{1}{2^{n-1}\pi} \int_B \frac{\nu_y \cdot (x-y)}{|x-y|^n} \mu(y) \mathrm{d}\sigma_y, \quad x \in D, \quad n = 2, 3. \tag{2.2}$$

Here, ν_y denotes the unit outward normal at $y \in B$, $\mathrm{d}\sigma_y$ denotes the boundary element, and $\mu \in C^2(B)$ denotes the density. The double-layer potential given by (2.2) satisfies (2.1a). To require that (2.2) satisfies (2.1b), we first recognize that it satisfies the following jump condition [14, 21]:

$$\lim_{\substack{x \to y^\star \in B \\ x \in D}} \frac{1}{2^{n-1}\pi} \int_B \frac{\nu_y \cdot (x-y)}{|x-y|^n} \mu(y) \mathrm{d}\sigma_y = \frac{1}{2^{n-1}\pi} \int_B \frac{\nu_y \cdot (y^\star - y)}{|y^\star - y|^n} \mu(y) \mathrm{d}\sigma_y - \frac{1}{2}\mu(y^\star). \tag{2.3}$$

In light of the jump condition (2.3) and the boundary condition (2.1b), μ satisfies the boundary integral equation:

$$\frac{1}{2^{n-1}\pi} \int_B \frac{\nu_y \cdot (y^\star - y)}{|y^\star - y|^n} \mu(y) \mathrm{d}\sigma_y - \frac{1}{2}\mu(y^\star) = f(y^\star), \quad y^\star \in B. \tag{2.4}$$

2.1. The close evaluation problem. The close evaluation problem refers to the large error resulting from computing the solution close to the boundary using a high-order quadrature rule at a fixed order. The close evaluation problem for (2.1) can be understood intuitively. Laplace's equation has no intrinsic finite length scale. This lack of finite length scale is manifest in the kernel of (2.4), which is singular at $y = y^\star$. When one introduces a finite discretization of the boundary, one effectively is introducing a finite length scale into the problem. Let Δs denote this finite length scale corresponding to the boundary discretization. For evaluation points in the domain farther than Δs from the boundary, the kernel of (2.2) is smooth, and a fixed Δs boundary discretization adequately resolves it. In contrast, for evaluation points in the domain closer than Δs from the boundary, the kernel is *nearly singular* and cannot be adequately resolved by this fixed boundary grid. Figure 1 shows these differences. This description of the close evaluation problem provides valuable insight. First, we understand that the size of the region exhibiting the close evaluation problem scales with the boundary discretization. Hence, in the limit, as the number of boundary points grows, this region shrinks proportionally, which is simply a consequence of the convergence of the numerical method. However, we also understand that *the close evaluation problem exists for any fixed boundary discretization* and is therefore unavoidable for any practical calculation.

As stated in the introduction, there have been several methods developed that successfully address the close evaluation problem. However, because the close evaluation problem is an intrinsic property of the boundary integral equation formulation and

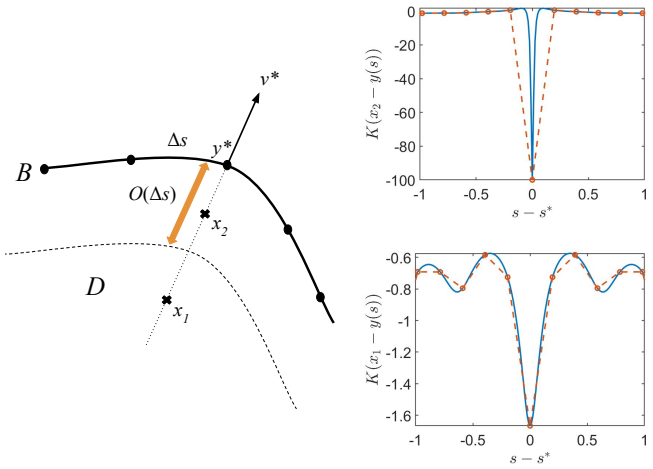

FIG. 1. *Two-dimensional sketch showing the finite length scale, Δs, of the discretization for (2.1) which leads to the close evaluation problem. For the point x_1 which is farther than Δs from the boundary, we find that the kernel is well resolved with the boundary grid. However, for the same boundary grid, we find that the kernel is poorly resolved for x_2, which is closer to the boundary than Δs. In each plot on the right, the kernel $K(x_i - y(s)) := \frac{\nu_y \cdot (x_i - y(s))}{|x_i - y(s)|^2}$, $i = 1, 2$, is plotted in blue, and a piecewise linear approximation using a fixed Δs grid is plotted in dashed orange.*

because close evaluations near the boundary are important for many physical applications, we are motivated to consider an alternative method to study the close evaluation problem. The method presented here closely follows the intuitive explanation above in which the discretization introduces a finite length scale into the problem. In particular, we apply asymptotic analysis to study the evaluation of the double-layer potential in the limit as the evaluation point x approaches a point on the boundary $y^\star$ and use this analysis to develop an accurate numerical method for these close evaluation points.

2.2. Preliminaries. To prepare to state our results of the asymptotic analysis, we introduce some notation. We refer the reader to Definition 1.1 ("Big-oh"), Definition 1.2 ("Big-oh" near z_0), Definition 1.4 ("Little-oh"), Definition 1.9 (Asymptotic sequence), and Definition 1.10 (Asymptotic expansion) from Miller's text [25] and to [16, section 2.5] for more details. Given some functions f and g defined over some set D, we will use the notation $f \ll g$ to indicate that $f(x) = o(g(x))$ whenever $x \in D$ and x tends to some $x_0 \in D$ [25, Definition 1.4]. Given a function f, we construct an asymptotic expansion of the form

$$f(x) \sim \sum_{n=0}^{\infty} \epsilon^n f_n(x), \quad \epsilon \to 0^+.$$

In other words, we only consider the asymptotic sequence $\{\epsilon^n\}_{n=0}^{\infty}$ as $\epsilon \to 0^+$ [25, Definition 1.10]. We will make use of the notation $f(x) = f_0(x) + \epsilon f_1(x) + O(\epsilon^2)$ to denote the "asymptotic approximation of $f(x)$ to order ϵ^2 in the limit as $\epsilon \to 0^+$." With these definitions and notations established, we state the formal asymptotic analysis in the next subsection.

2.3. Results of asymptotic analysis. To study the close evaluation of (2.2), we introduce the parameter ϵ in the evaluation point x according to

$$x = y^\star - \epsilon \ell \nu^\star \tag{2.5}$$

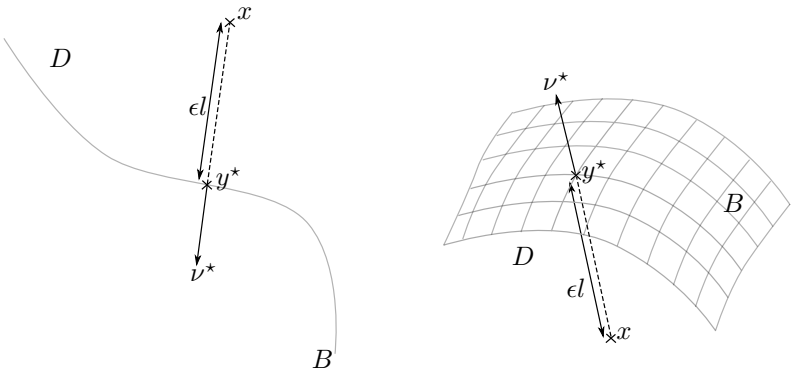

FIG. 2. *Sketch of the quantities introduced in* (2.5) *to study evaluation points close to the boundary in two dimensions (left) and in three dimensions (right).*

and consider the asymptotic limit of $\epsilon \to 0^+$. Here, $y^\star \in B$ denotes the closest point to x on the boundary; $\nu^\star$ denotes the unit, outward normal at $y^\star$; and ℓ denotes a characteristic length of the problem, like the radius of curvature at $y^\star$ (see Figure 2). Since the solution of (2.1) continuously approaches its boundary data from within D,

$$u(x) = u(y^\star - \epsilon\ell\nu^\star) = f(y^\star) + \epsilon U(y^\star;\epsilon). \tag{2.6}$$

To determine an expression for U, we substitute (2.2) evaluated at (2.5) for $u(y^\star - \epsilon\ell\nu^\star)$ and (2.4) for $f(y^\star)$ into (2.6) and find that

$$U(y^\star;\epsilon) = \epsilon^{-1}\left[\frac{1}{2}\mu(y^\star) + \frac{1}{2^{n-1}\pi}\int_B \left[\frac{\nu_y\cdot(y_d-\epsilon\ell\nu^\star)}{|y_d-\epsilon\ell\nu^\star|^n} - \frac{\nu_y\cdot y_d}{|y_d|^n}\right]\mu(y)\mathrm{d}\sigma_y\right], \tag{2.7}$$

where we have introduced the notation, $y_d = y^\star - y$. Next, we make use of Gauss's theorem [14],

$$\frac{1}{2^{n-1}\pi}\int_B \frac{\nu_y\cdot(x-y)}{|x-y|^n}\mathrm{d}\sigma_y = \begin{cases} -1 & x\in D,\\ -\frac{1}{2} & x\in B,\\ 0 & x\notin \bar{D}, \end{cases} \tag{2.8}$$

to write

$$\begin{aligned}\frac{1}{2}\mu(y^\star) &= \mu(y^\star) - \frac{1}{2}\mu(y^\star)\\ &= -\frac{1}{2^{n-1}\pi}\int_B \frac{\nu_y\cdot(y_d-\epsilon\ell\nu^\star)}{|y_d-\epsilon\ell\nu^\star|^n}\mu(y^\star)\mathrm{d}\sigma_y + \frac{1}{2^{n-1}\pi}\int_B \frac{\nu_y\cdot y_d}{|y_d|^n}\mu(y^\star)\mathrm{d}\sigma_y.\end{aligned} \tag{2.9}$$

Substituting (2.9) into (2.7) yields

$$U(y^\star;\epsilon) = \frac{1}{2^{n-1}\pi}\int_B \epsilon^{-1}\left[\frac{\nu_y\cdot(y_d-\epsilon\ell\nu^\star)}{|y_d-\epsilon\ell\nu^\star|^n} - \frac{\nu_y\cdot y_d}{|y_d|^n}\right][\mu(y)-\mu(y^\star)]\mathrm{d}\sigma_y. \tag{2.10}$$

Let

$$\mathcal{K}(y_d,\epsilon) = \frac{1}{2^{n-1}\pi}\frac{\nu_y\cdot(y_d-\epsilon l\nu^\star)}{|y_d-\epsilon l\nu^\star|^n}. \tag{2.11}$$

Then (2.10) can be rewritten as

$$U(y^\star;\epsilon) = \int_B \frac{\mathcal{K}(y_d,\epsilon)-\mathcal{K}(y_d,0)}{\epsilon}[\mu(y)-\mu(y^\star)]\mathrm{d}\sigma_y, \tag{2.12}$$

which reveals that the kernel of $U(y^\star;\epsilon)$ is proportional to $\partial_\epsilon \mathcal{K}(y_d,0)$. This observation motivates us to seek asymptotic expansions for $U(y^\star;\epsilon)$. Note that $U(y^\star;\epsilon)$ is a weakly singular integral that provides an important contribution to the double-layer potential off and on the boundary. The asymptotic analysis results of this paper are stated in the two conjectures below.

CONJECTURE 2.1 (two-dimensional asymptotic approximation). *Consider a bounded open set $D \subset \mathbb{R}^2$ with an analytic closed boundary B that can be parameterized as $y = y(t)$ for $0 \le t \le 2\pi$. Let $y^\star = y(0)$. For $f \in \mathcal{C}^2(B)$, the solution of (2.1) at $x = y^\star - \epsilon\ell\nu^\star$ is given by $u(y^\star - \epsilon\ell\nu^\star) = f(y^\star) + \epsilon U(y^\star;\epsilon)$, and the asymptotic approximation of $U(y^\star;\epsilon)$ to $O(\epsilon^2)$ is*

$$U(y^\star;\epsilon) = L_1[\mu](y^\star) + \epsilon L_2[\mu](y^\star) - \epsilon \frac{\ell^2 y'(0)\cdot y''(0)}{4|y'(0)|^4}\frac{\mathrm{d}\mu(y(t))}{\mathrm{d}t}\bigg|_{t=0} + \epsilon\frac{\ell^2}{4|y'(0)|^2}\frac{\mathrm{d}^2\mu(y(t))}{\mathrm{d}t^2}\bigg|_{t=0} + O(\epsilon^2) \tag{2.13}$$

with

$$L_1[\mu](y^\star) = \ell\int_B \frac{2(\nu_y\cdot y_d)(\nu^\star\cdot y_d) - \nu_y\cdot\nu^\star|y_d|^2}{|y_d|^4}\,[\mu(y)-\mu(y^\star)]\,\mathrm{d}\sigma_y \tag{2.14}$$

and

$$L_2[\mu](y^\star) = \ell^2\int_B \frac{(\nu_y\cdot y_d)\left[4(\nu^\star\cdot y_d)^2\right] - 2|y_d|^2(\nu_y\cdot\nu^\star)(\nu^\star\cdot y_d)}{|y_d|^6}\,[\mu(y)-\mu(y^\star)]\,\mathrm{d}\sigma_y. \tag{2.15}$$

By replacing U in $u(y^\star - \epsilon\ell\nu^\star) = f(y^\star) + \epsilon U(y^\star;\epsilon)$ with (2.13), we obtain the asymptotic approximation of $u(y^\star - \epsilon\ell\nu^\star)$ to $O(\epsilon^3)$.

CONJECTURE 2.2 (three-dimensional asymptotic approximation). *Consider a bounded open set $D \subset \mathbb{R}^3$ with an analytic closed and oriented surface B that can be mapped to S^2 via an analytic diffeomorphism and that can be parameterized as $y = y(s,t)$ for $s \in [0,\pi]$, $t \in [-\pi,\pi]$. Let $y^\star = y(0,\cdot) = \lim_{\theta\to 0^+}\frac{1}{2\pi}\int_{-\pi}^{\pi} y(\theta,\varphi)\mathrm{d}\varphi$ be the spherical mean. For $f \in \mathcal{C}^2(B)$, the solution of (2.1) at $x = y^\star - \epsilon\ell\nu^\star$ is given by $u(y^\star - \epsilon\ell\nu^\star) = f(y^\star) + \epsilon U(y^\star;\epsilon)$, and the asymptotic approximation of $U(y^\star;\epsilon)$ to $O(\epsilon)$ is*

$$U(y^\star;\epsilon) = L_1[\mu](y^\star) + O(\epsilon) \tag{2.16}$$

with

$$L_1[\mu](y^\star) = \ell\int_B \frac{3(\nu_y\cdot y_d)(\nu^\star\cdot y_d) - |y_d|^2\nu_y\cdot\nu^\star}{|y_d|^5}\,[\mu(y)-\mu(y^\star)]\,\mathrm{d}\sigma_y. \tag{2.17}$$

By replacing U in $u(y^\star - \epsilon\ell\nu^\star) = f(y^\star) + \epsilon U(y^\star;\epsilon)$ with (2.16), we obtain the asymptotic approximation of $u(y^\star - \epsilon\ell\nu^\star)$ to $O(\epsilon^2)$.

We give the following remarks:

• We consider smooth boundaries (analytic, closed) for which we can have an explicit parameterization. Note that the parameterization enables us to work with integrals defined on a circle or a sphere. In other words the results hold for any boundary that can be mapped to S^{n-1} via an analytic diffeomorphism. Denoting this diffeomorphism by $\psi : S^{n-1} \to B$, we consider the parameterization $y = \psi \circ y_{S^{n-1}}$ with $y_{S^{n-1}}$ denoting the parameterization defined on S^{n-1}. In principle, one could

extend similar results on patches by locally applying some mapping to an arc or a spherical cap. However, this extension is not within the scope of this paper.

• One could obtain higher-order results provided that $f, \mu \in \mathcal{C}^k(B)$ for $k > 2$. On the other hand, one could investigate the problem with less required regularity. However, we do not investigate that aspect of the problem here. In what follows, we take advantage of spectral methods to compute higher-order derivatives.

• As is shown in the next sections, computations to obtain asymptotic approximations can be tedious, especially for higher-order terms, and for the three-dimensional case. It is for this reason that we only consider the $O(\epsilon^2)$ approximation for the three-dimensional case.

• In Conjecture 2.1, results are written for $y^\star$ being at $t = 0$ for simplicity. However, these results hold for any $y^\star = y(t^\star)$ with $t^\star \in [0, 2\pi]$ through a rotation. Denoting this rotation by $R : S^1 \to S^1$, we then consider $y := R \circ \psi \circ y_{S^1}$.

• Similarly, in Conjecture 2.2, results are written for $y^\star$ situated at the north pole ($s = 0$) of the unit sphere. For other evaluation points, one simply rotates the coordinate system to arrive at this configuration. Details for this rotation can be found in Appendix B.

• From a numerical point of view, it is desirable to achieve spectral accuracy for μ, so that the main source of error is due to the close evaluation of the double-layer potential. When this is done, we compute derivatives of μ needed for the two-dimensional asymptotic approximation using spectral differentiation methods.

The next two sections give a derivation of these two conjectures based on a careful and systematic asymptotic analysis. This derivation is formal because we do not rigorously prove one technical point in it. This technicality is discussed in detail for the specific case of the unit circle in Appendix A, where calculations are explicit and the proof is given. Rather than focus on the technicalities for general cases, we proceed with these two conjectures, develop new numerical methods based on them, and test their accuracy on several examples. Since we make use of explicit parameterization for B, we consider the two- and three-dimensional problems separately.

3. Asymptotic approximations in two dimensions. We give a derivation of the $O(\epsilon)$ term in Conjecture 2.1, i.e., $L_1[\mu](y^\star)$ defined in (2.14), and then comment on how to compute the $O(\epsilon^2)$ terms in Conjecture 2.1. As stated in Conjecture 2.1, we assume B to be an analytic, closed curve on the plane. We introduce the parameter $t \in [-\pi, \pi]$ such that $y = y(t)$ and $y^\star = y(0)$. In terms of this parameterization, (2.10) is given by

$$U(y^\star; \epsilon) = \frac{1}{2\pi} \int_{-\pi}^{\pi} \epsilon^{-1} K(t; \epsilon)[\tilde{\mu}(t) - \tilde{\mu}(0)] \mathrm{d}t \tag{3.1}$$

with $\tilde{\mu}(t) = \mu(y(t))$ and $\tilde{\mu}(0) = \mu(y(0)) = \mu(y^\star)$ and

$$K(t; \epsilon) = \left[\frac{\tilde{\nu}(t) \cdot (y_d(t) - \epsilon \ell \nu^\star)}{|y_d(t) - \epsilon \ell \nu^\star|^2} - \frac{\tilde{\nu}(t) \cdot y_d(t)}{|y_d(t)|^2} \right] J(t) \tag{3.2}$$

with $\tilde{\nu}(t) = \nu(y(t))$, $y_d(t) = y(0) - y(t)$, and $J(t) = |y'(t)|$. Note that $\nu^\star = \tilde{\nu}(0)$.

To determine the asymptotic expansion for U, we write

$$U(y^\star; \epsilon) = U^{\text{in}}(y^\star; \epsilon) + U^{\text{out}}(y^\star; \epsilon) \tag{3.3}$$

with the inner expansion, U^{in}, and the outer expansion, U^{out}, given by

$$U^{\text{in}}(y^\star;\epsilon) = \frac{1}{2\pi}\int_{-\sqrt{\epsilon}/2}^{\sqrt{\epsilon}/2} \epsilon^{-1}K(t;\epsilon)\,[\tilde{\mu}(t)-\tilde{\mu}(0)]\,\mathrm{d}t, \tag{3.4a}$$

$$\begin{aligned} U^{\text{out}}(y^\star;\epsilon) = \frac{1}{2\pi}\int_{-\pi}^{-\sqrt{\epsilon}/2} \epsilon^{-1}K(t;\epsilon)\,[\tilde{\mu}(t)-\tilde{\mu}(0)]\,\mathrm{d}t \\ + \frac{1}{2\pi}\int_{\sqrt{\epsilon}/2}^{\pi} \epsilon^{-1}K(t;\epsilon)\,[\tilde{\mu}(t)-\tilde{\mu}(0)]\,\mathrm{d}t. \end{aligned} \tag{3.4b}$$

The inner expansion involves integration over an $O(\epsilon^{1/2})$ portion of the boundary about $y^\star$, whereas the outer expansion involves integration over the remaining portion of the boundary. The following results also hold if one considers an $O(\epsilon^\alpha)$ portion of the boundary with $0<\alpha<1$. Since the inner and outer expansions come from splitting the integral over the boundary, we refer to this procedure as an *integral splitting method* for computing the asymptotic expansion for the close evaluation of the double-layer potential.

We determine the leading-order asymptotic behaviors of U^{in} and U^{out} in the subsections below. Then, we combine those results to obtain the asymptotic approximation for the double-layer potential in two dimensions and discuss higher-order asymptotic approximations. The procedure we use here follows that by Hinch [16, section 3]. We have developed *Mathematica* notebooks that contain the presented calculations, available in a GitHub repository [19]. In what follows we assume that K and $\tilde{\mu}$ have asymptotic expansions in the limit as $\epsilon\to 0^+$ (as described in section 2.2) and that the remainder of the asymptotic approximation to $O(\epsilon^n)$ with $n>1$ yields an $O(\epsilon^{n-1})$ after integration. Details of the proof are given for the unit circle in Appendix A.

3.1. Inner expansion. To determine the leading-order asymptotic behavior of U^{in}, we substitute $t=\epsilon T$ into (3.4a) and obtain

$$U^{\text{in}}(y^\star;\epsilon) = \frac{1}{2\pi}\int_{-1/(2\sqrt{\epsilon})}^{1/(2\sqrt{\epsilon})} K(\epsilon T;\epsilon)\,[\tilde{\mu}(\epsilon T)-\tilde{\mu}(0)]\,\mathrm{d}T. \tag{3.5}$$

Recognizing that $\tilde{\nu}(\epsilon T)=\nu^\star+O(\epsilon)$ and $y_d(\epsilon T)=-\epsilon T y'(0)+O(\epsilon^2)$ with $\nu^\star\cdot y'(0)=0$, we find by expanding $K(\epsilon T;\epsilon)$ about $\epsilon=0$ that

$$K(\epsilon T;\epsilon) = -\frac{\epsilon^{-1}\ell J(0)}{T^2J^2(0)+\ell^2}+O(1). \tag{3.6}$$

Using the fact that this leading-order behavior is even in T and expanding $\tilde{\mu}$ about $\epsilon=0$, we substitute these expansions into (3.5) to get

$$\begin{aligned} U^{\text{in}}(y^\star;\epsilon) &= \frac{1}{2\pi}\int_{-1/(2\sqrt{\epsilon})}^{1/(2\sqrt{\epsilon})} \left[-\frac{\epsilon^{-1}\ell J(0)}{T^2J^2(0)+\ell^2}+O(1)\right][\tilde{\mu}(\epsilon T)-\tilde{\mu}(0)]\,\mathrm{d}T \\ &= \frac{1}{2\pi}\int_{0}^{1/(2\sqrt{\epsilon})} \left[-\frac{\epsilon^{-1}\ell J(0)}{T^2J^2(0)+\ell^2}+O(1)\right][\tilde{\mu}(\epsilon T)+\tilde{\mu}(-\epsilon T)-2\tilde{\mu}(0)]\,\mathrm{d}T \\ &= \frac{1}{2\pi}\int_{0}^{1/(2\sqrt{\epsilon})} \left[-\frac{\epsilon^{-1}\ell J(0)}{T^2J^2(0)+\ell^2}+O(1)\right][\epsilon^2T^2\tilde{\mu}''(0)+O(\epsilon^4)]\,\mathrm{d}T \\ &= \frac{1}{2\pi}\int_{0}^{1/(2\sqrt{\epsilon})} \left[-\frac{\epsilon T^2\ell J(0)}{T^2J^2(0)+\ell^2}\tilde{\mu}''(0)+O(\epsilon^2)\right]\mathrm{d}T. \end{aligned} \tag{3.7}$$

Above, we have obtained an asymptotic approximation of the integrand to $O(\epsilon^2)$ (see section 2.2). Following the procedure given by Hinch [16, section 3.4], after integrating (see [19] and Appendix A) and expanding about $\epsilon = 0$, we find the leading-order asymptotic behavior of U^{in} to be

$$U^{\text{in}}(y^\star;\epsilon) = -\frac{\sqrt{\epsilon}\ell}{4\pi J(0)}\tilde{\mu}''(0) + O(\epsilon). \tag{3.8}$$

Remark 1. The obtained asymptotic expansion used in (3.7) is nonuniform. One needs to establish uniform convergence to rigorously prove that the remainder of the asymptotic approximation to order ϵ^2, after integration, is $O(\epsilon)$. Obtaining this result in general is not straightforward. We give details of the proof for the case of the unit circle in Appendix A.

3.2. Outer expansion. To determine the leading-order asymptotic behavior of U^{out}, we expand $K(t;\epsilon)$ about $\epsilon = 0$ and find that $K(t;\epsilon) = [\epsilon K_1(t) + O(\epsilon^2)]J(t)$ with

$$K_1(t) = \ell\frac{2(\tilde{\nu}(t)\cdot y_d(t))(\nu^\star \cdot y_d(t)) - \tilde{\nu}(t)\cdot\nu^\star|y_d(t)|^2}{|y_d(t)|^4}. \tag{3.9}$$

Substituting this expansion into (3.4b), we find that

$$\begin{aligned} U^{\text{out}}(y^\star;\epsilon) = \frac{1}{2\pi}\int_{-\pi}^{-\sqrt{\epsilon}/2} K_1(t)\left[\tilde{\mu}(t) - \tilde{\mu}(0)\right]J(t)\mathrm{d}t \\ + \frac{1}{2\pi}\int_{\sqrt{\epsilon}/2}^{\pi} K_1(t)\left[\tilde{\mu}(t) - \tilde{\mu}(0)\right]J(t)\mathrm{d}t + O(\epsilon). \end{aligned} \tag{3.10}$$

To eliminate $\sqrt{\epsilon}$ from the integration limits, we rewrite (3.10) as

$$U^{\text{out}}(y^\star;\epsilon) = \frac{1}{2\pi}\int_{-\pi}^{\pi} K_1(t)\left[\tilde{\mu}(t) - \tilde{\mu}(0)\right]J(t)\mathrm{d}t - V^{\text{out}}(y^\star;\epsilon) + O(\epsilon) \tag{3.11}$$

with

$$V^{\text{out}}(y^\star;\epsilon) = \frac{1}{2\pi}\int_{-\sqrt{\epsilon}/2}^{\sqrt{\epsilon}/2} K_1(t)\left[\tilde{\mu}(t) - \tilde{\mu}(0)\right]J(t)\mathrm{d}t. \tag{3.12}$$

Note that $t \mapsto K_1(t)\left[\tilde{\mu}(t) - \tilde{\mu}(0)\right]J(t)$ can be integrated, as a Cauchy principal value, allowing us to write (3.11) with (3.12).

To determine the leading-order behavior for V^{out}, we proceed exactly as in section 3.1. We substitute $t = \epsilon T$ into (3.12) and obtain

$$V^{\text{out}}(y^\star;\epsilon) = \frac{1}{2\pi}\int_{-1/(2\sqrt{\epsilon})}^{1/(2\sqrt{\epsilon})} K_1(\epsilon T)\left[\tilde{\mu}(\epsilon T) - \tilde{\mu}(0)\right]J(\epsilon T)\epsilon\mathrm{d}T. \tag{3.13}$$

Again, by recognizing that $\tilde{\nu}(\epsilon T) = \nu^\star + O(\epsilon)$ and $y_d(\epsilon T) = -\epsilon T y'(0) + O(\epsilon^2)$ with $\nu^\star \cdot y'(0) = 0$, we find that

$$K_1(\epsilon T) = -\frac{\epsilon^{-2}\ell}{T^2 J^2(0)} + O(\epsilon^{-1}). \tag{3.14}$$

Using the fact that this leading-order behavior is even in T and that $J(\epsilon T) = J(0) + O(\epsilon)$, when we substitute it into (3.13), we find, after expanding about $\epsilon = 0$, that

(3.15)
$$\begin{aligned}
V^{\text{out}}(y^\star;\epsilon) &= \frac{1}{2\pi}\int_{-1/(2\sqrt{\epsilon})}^{1/(2\sqrt{\epsilon})} \left[-\frac{\epsilon^{-2}\ell}{T^2J^2(0)} + O(\epsilon^{-1})\right] [\tilde{\mu}(\epsilon T) - \tilde{\mu}(0)]\, J(\epsilon T)\epsilon \mathrm{d}T \\
&= \frac{1}{2\pi}\int_{0}^{1/(2\sqrt{\epsilon})} \left[-\frac{\epsilon^{-2}\ell}{T^2J^2(0)} + O(\epsilon^{-1})\right] [\tilde{\mu}(\epsilon T) + \tilde{\mu}(-\epsilon T) - 2\tilde{\mu}(0)]\, [J(0) + O(\epsilon)]\, \epsilon \mathrm{d}T \\
&= \frac{1}{2\pi}\int_{0}^{1/(2\sqrt{\epsilon})} \left[-\frac{\epsilon^{-1}\ell}{T^2J(0)} + O(1)\right] \left[\epsilon^2T^2\tilde{\mu}''(0) + O(\epsilon^4)\right] \mathrm{d}T \\
&= \frac{1}{2\pi}\int_{0}^{1/(2\sqrt{\epsilon})} \left[-\frac{\epsilon\ell}{J(0)}\tilde{\mu}''(0) + O(\epsilon^2)\right] \mathrm{d}T \\
&= -\frac{\sqrt{\epsilon}\ell}{4\pi J(0)}\tilde{\mu}''(0) + O(\epsilon).
\end{aligned}$$

Substituting this result into (3.11), we find that the leading-order asymptotic behavior for U^{out} is given by

$$U^{\text{out}}(y^\star;\epsilon) = \frac{1}{2\pi}\int_{-\pi}^{\pi} K_1(t)\, [\tilde{\mu}(t) - \tilde{\mu}(0)]\, J(t)\mathrm{d}t + \frac{\sqrt{\epsilon}\ell}{4\pi J(0)}\tilde{\mu}''(0) + O(\epsilon). \tag{3.16}$$

3.3. Two-dimensional asymptotic approximation. We obtain an asymptotic approximation for U by summing the leading-order behaviors obtained for U^{in} and U^{out} given in (3.8) and (3.16), respectively, which gives

$$U(y^\star;\epsilon) = \frac{1}{2\pi}\int_{-\pi}^{\pi} K_1(t)\, [\tilde{\mu}(t) - \tilde{\mu}(0)]\, J(t)\mathrm{d}t + O(\epsilon) := L_1[\mu] + O(\epsilon), \tag{3.17}$$

where K_1 is given by (3.9). It follows that the asymptotic approximation for $u(y^\star - \epsilon\ell\nu^\star)$ to $O(\epsilon^2)$ is

$$u(y^\star - \epsilon\ell\nu^\star) = f(y^\star) + \epsilon L_1[\mu] + O(\epsilon^2). \tag{3.18}$$

This result gives the leading-order asymptotic behavior of $U(y^\star;\epsilon)$ as $\epsilon \to 0^+$. The obtained asymptotic approximation does not have any terms of $O(\epsilon^{1/2})$ because those terms in (3.8) and (3.16) vanish identically. Asymptotic approximation (3.18) gives an explicit approximation for the close evaluation of the double-layer potential in two dimensions. According to the asymptotic analysis, the expected error of this approximation is $O(\epsilon^2)$. It gives the double-layer potential as the Dirichlet data at the boundary point $y^\star$ closest to the evaluation point x plus a nonlocal correction. This nonlocal correction is consistent with the fact that solutions to elliptic partial differential equations have a global dependence on their boundary data. The leading-order asymptotic expansion indicates that the nonlocal correction only comes from the outer expansion, and the inner expansion does not contribute to the lower-order terms.

As stated in Remark 1, we do not establish the uniform convergence that is needed to rigorously justify this asymptotic error, and we proceed with this asymptotic analysis as conjecture. We show in the numerical examples below that this expression yields approximations with the expected asymptotic error estimate, thereby indicating that the conjecture is correct.

3.4. Higher-order asymptotic approximations. By continuing on to higher-order terms in the expansions for U^{in} and U^{out}, we can obtain higher-order asymptotic approximations. Details can be found in the *Mathematica* notebooks [19]. The result from these calculations is the asymptotic approximation

$$U(y^\star;\epsilon) = L_1[\mu] + \epsilon\left[L_2[\mu] - \frac{\ell^2 y'(0)\cdot y''(0)}{4J^4(0)}\tilde{\mu}'(0) + \frac{\ell^2}{4J^2(0)}\tilde{\mu}''(0)\right] + O(\epsilon^2) \tag{3.19}$$

with $L_1[\mu]$ as in (3.17) and

$$L_2[\mu] := \frac{1}{2\pi}\int_{-\pi}^{\pi} K_2(t)\left[\tilde{\mu}(t) - \tilde{\mu}(0)\right] J(t)\mathrm{d}t, \tag{3.20}$$

where

$$K_2(t) = \ell^2 \frac{(\nu\cdot y_d)\left[4(\nu^\star\cdot y_d)^2 - |y_d|^2\right] - 2|y_d|^2(\nu\cdot\nu^\star)(\nu^\star\cdot y_d)}{|y_d|^6}. \tag{3.21}$$

It follows that the asymptotic approximation for $u(y^\star - \epsilon\ell\nu^\star)$ to $O(\epsilon^3)$ is given by

$$\begin{aligned} u(y^\star - \epsilon\ell\nu^\star) &= f(y^\star) + \epsilon L_1[\mu] \\ &\quad + \epsilon^2\left[L_2[\mu] - \frac{\ell^2 y'(0)\cdot y''(0)}{4J^4(0)}\tilde{\mu}'(0) + \frac{\ell^2}{4J^2(0)}\tilde{\mu}''(0)\right] + O(\epsilon^3). \end{aligned} \tag{3.22}$$

In addition to nonlocal terms, this approximation includes local contributions made by first and second derivatives of the density, μ, evaluated at the boundary point $y^\star$. These local contributions come from the inner expansion.

4. Asymptotic approximations in three dimensions. As stated in Conjecture 2.2, we assume B to be an analytic, closed, and oriented surface that can be parameterized by $y = y(s,t)$ for $s \in [0,\pi]$ and $t \in [-\pi,\pi]$. This implies that the double-layer potential is a surface integral in a spherical coordinate system, which we will explicitly make use of in what follows. We assume that $y(s,-\pi) = y(s,\pi)$ $\forall s \in [0,\pi]$ and that $y^\star = y(0,\cdot)$, where $y(0,\cdot) := \lim_{\theta\to 0^+}\frac{1}{2\pi}\int_{-\pi}^{\pi} y(\theta,\varphi)\mathrm{d}\varphi$ denotes the spherical mean. In other words, we consider $y^\star$ to be at the north pole of the sphere corresponding to $s = 0$. One can always arrive at this configuration by rotating the local spherical system (see Appendix B). In terms of this parameterization, (2.10) is given by

$$U(y^\star;\epsilon) = \frac{1}{4\pi}\int_{-\pi}^{\pi}\int_{0}^{\pi} \epsilon^{-1}K(s,t;\epsilon)\left[\tilde{\mu}(s,t) - \tilde{\mu}(0,\cdot)\right]\sin(s)\mathrm{d}s\mathrm{d}t \tag{4.1}$$

with $\tilde{\mu}(s,t) = \mu(y(s,t))$ and $\tilde{\mu}(0,\cdot) = \mu(y(0,\cdot))$ and

$$K(s,t;\epsilon) = \left[\frac{\tilde{\nu}(s,t)\cdot(y_d(s,t) - \epsilon\ell\nu^\star)}{|y_d(s,t) - \epsilon\ell\nu^\star|^3} - \frac{\tilde{\nu}(s,t)\cdot y_d(s,t)}{|y_d(s,t)|^3}\right] J(s,t) \tag{4.2}$$

with $\tilde{\nu}(s,t) = \nu_y$, $y_d(s,t) = y(0,\cdot) - y(s,t)$, and $J(s,t) = |y_s(s,t)\times y_t(s,t)|/\sin(s)$. The integral (4.1) is written as a surface integral in a spherical coordinate system. In this integral, we have explicitly included the spherical Jacobian, $\sin(s)$. It follows that $J(s,t)\sin(s)$ for this integral is always bounded. Note also that $\nu^\star = \tilde{\nu}(0,\cdot)$. Write

$$U(y^\star;\epsilon) = U^{\text{in}}(y^\star;\epsilon) + U^{\text{out}}(y^\star;\epsilon) \tag{4.3}$$

with the inner expansion, U^{in}, and the outer expansion, U^{out}, given by

$$U^{\text{in}}(y^\star;\epsilon) = \frac{1}{4\pi}\int_{-\pi}^{\pi}\int_{0}^{\sqrt{\epsilon}} \epsilon^{-1}K(s,t;\epsilon)\left[\tilde{\mu}(s,t)-\tilde{\mu}(0,\cdot)\right]\sin(s)\mathrm{d}s\mathrm{d}t, \tag{4.4a}$$

$$U^{\text{out}}(y^\star;\epsilon) = \frac{1}{4\pi}\int_{-\pi}^{\pi}\int_{\sqrt{\epsilon}}^{\pi} \epsilon^{-1}K(s,t;\epsilon)\left[\tilde{\mu}(s,t)-\tilde{\mu}(0,\cdot)\right]\sin(s)\mathrm{d}s\mathrm{d}t. \tag{4.4b}$$

We once again assume that K and μ have asymptotic expansions as $\epsilon \to 0^+$ and that the remainder of the asymptotic approximation to $O(\epsilon^n)$ with $n > 1$ is $O(\epsilon^{n-1})$ after integration. We determine the leading-order asymptotic behaviors for U^{in} and U^{out} separately. Then, we combine those results to obtain an asymptotic approximation for the close evaluation of the double-layer potential in three dimensions and discuss higher-order asymptotic approximations. The procedure follows [16, section 3]. Details can be found in the *Mathematica* notebook available on GitHub [19].

4.1. Inner expansion. To find the leading-order asymptotic behavior of U^{in}, we substitute $s = \epsilon S$ into (4.4a) and obtain

$$U^{\text{in}}(y^\star;\epsilon) = \frac{1}{4\pi}\int_{-\pi}^{\pi}\int_{0}^{1/\sqrt{\epsilon}} K(\epsilon S,t;\epsilon)\left[\tilde{\mu}(\epsilon S,t)-\tilde{\mu}(0,\cdot)\right]\sin(\epsilon S)\mathrm{d}S\mathrm{d}t. \tag{4.5}$$

Recognizing that $\tilde{\nu}(\epsilon S,t) = \nu^\star + O(\epsilon)$ and $y_d(\epsilon S,t) = -\epsilon S y_s(0,\cdot) + O(\epsilon^2)$ with the vector $y_s(0,\cdot)$ lying on the plane tangent to B at $y^\star$, we find by expanding $K(\epsilon S,t;\epsilon)$ about $\epsilon = 0$ that

$$K(\epsilon S,t;\epsilon) = -\frac{\epsilon^{-2}\ell J(0,\cdot)}{(S^2|y_s(0,\cdot)|^2+\ell^2)^{3/2}} + O(\epsilon^{-1}). \tag{4.6}$$

Since this leading-order asymptotic behavior for $K(\epsilon S,t;\epsilon)$ is independent of t, we write

$$\begin{aligned} U^{\text{in}}(y^\star;\epsilon) = \frac{1}{4\pi}\int_{0}^{\pi}\int_{0}^{1/\sqrt{\epsilon}} &\left[-\frac{\epsilon^{-2}\ell J(0,\cdot)}{(S^2|y_s(0,\cdot)|^2+\ell^2)^{3/2}} + O(\epsilon^{-1})\right] \\ &\left[\tilde{\mu}(\epsilon S,t)+\tilde{\mu}(\epsilon S,t+\pi)-2\tilde{\mu}(0,\cdot)\right]\sin(\epsilon S)\mathrm{d}S\mathrm{d}t. \end{aligned} \tag{4.7}$$

Next, we use the regularity of $\tilde{\mu}$ over the north pole to substitute $\tilde{\mu}(\epsilon S,t+\pi) = \tilde{\mu}(-\epsilon S,t)$ so that

$$\begin{aligned} \tilde{\mu}(\epsilon S,t)+\tilde{\mu}(\epsilon S,t+\pi)-2\tilde{\mu}(0,\cdot) &= \tilde{\mu}(\epsilon S,t)+\tilde{\mu}(-\epsilon S,t)-2\tilde{\mu}(0,\cdot) \\ &= \epsilon^2 S^2\tilde{\mu}_{ss}(0,\cdot)+O(\epsilon^4). \end{aligned} \tag{4.8}$$

Thus, we find after substituting (4.8) and $\sin(\epsilon S) = \epsilon S + O(\epsilon^3)$ into (4.7) that

$$\begin{aligned} U^{\text{in}}(y^\star;\epsilon) &= \frac{1}{4\pi}\int_{0}^{\pi}\int_{0}^{1/\sqrt{\epsilon}}\left[-\frac{\epsilon S^3\ell J(0,\cdot)}{(S^2|y_s(0,\cdot)|^2+\ell^2)^{3/2}}\tilde{\mu}_{ss}(0,\cdot)+O(\epsilon^2)\right]\mathrm{d}S\mathrm{d}t \\ &= -\frac{\ell J(0,\cdot)}{8}\Delta_{S^2}\mu(y^\star)\int_{0}^{1/\sqrt{\epsilon}}\left[\frac{\epsilon S^3}{(S^2|y_s(0,\cdot)|^2+\ell^2)^{3/2}}+O(\epsilon^2)\right]\mathrm{d}S, \end{aligned} \tag{4.9}$$

where we have used the fact that

$$\frac{1}{\pi}\int_{0}^{\pi}\tilde{\mu}_{ss}(0,\cdot)\mathrm{d}t = \frac{1}{2}\Delta_{S^2}\mu(y^\star) \tag{4.10}$$

with $\Delta_{S^2}\mu(y^\star)$ denoting the spherical Laplacian of μ evaluated at $y^\star$ (see Appendix C). Note that the Laplace–Beltrami operator Δ_{S^2} appears due to the use of a local spherical coordinate system. Furthermore, following the procedure given by Hinch [16, section 3.4] (see [19] and Appendix A), when expanding about $\epsilon = 0$, we have

$$\int_0^{1/\sqrt{\epsilon}} \left[\frac{\epsilon S^3}{(S^2|y_s(0,\cdot)|^2 + \ell^2)^{3/2}} + O(\epsilon^2) \right] \mathrm{d}S = \frac{\sqrt{\epsilon}}{|y_s(0,\cdot)|^3} + O(\epsilon), \tag{4.11}$$

and therefore

$$U^{\mathrm{in}}(y^\star;\epsilon,\delta) = -\frac{\sqrt{\epsilon}\ell J(0,\cdot)}{8|y_s(0,\cdot)|^3}\Delta_{S^2}\mu(y^\star) + O(\epsilon). \tag{4.12}$$

This result gives the leading-order asymptotic behavior of U^{in}.

Remark 2. One needs again to establish uniform convergence to rigorously prove that the remainder of the asymptotic approximation to $O(\epsilon^2)$, after integration, is $O(\epsilon)$. One could obtain the results in the case of the unit sphere, proceeding similarly as in Appendix A.

4.2. Outer expansion. To determine the leading-order asymptotic behavior of U^{out}, we expand $K(s,t;\epsilon)$ about $\epsilon = 0$ and find $K(s,t;\epsilon) = \left[\epsilon K_1(s,t) + O(\epsilon^2)\right] J(s,t)$ with

$$K_1(s,t) = \ell \frac{3(\tilde{\nu}(s,t)\cdot y_d(s,t))(\nu^\star \cdot y_d(s,t)) - |y_d(s,t)|^2 \tilde{\nu}(s,t)\cdot\nu^\star}{|y_d(s,t)|^5}. \tag{4.13}$$

Substituting this expansion into (4.4b), we obtain

$$U^{\mathrm{out}}(y^\star;\epsilon) = \frac{1}{4\pi}\int_{-\pi}^{\pi}\int_{\sqrt{\epsilon}}^{\pi} K_1(s,t)\left[\tilde{\mu}(s,t) - \tilde{\mu}(0,\cdot)\right] J(s,t)\sin(s)\mathrm{d}s\mathrm{d}t + O(\epsilon). \tag{4.14}$$

To eliminate $\sqrt{\epsilon}$ as a limit of integration in (4.14), we write

$$U^{\mathrm{out}}(y^\star;\epsilon) = \frac{1}{4\pi}\int_{-\pi}^{\pi}\int_{0}^{\pi} K_1(s,t)\left[\tilde{\mu}(s,t) - \tilde{\mu}(0,\cdot)\right] J(s,t)\sin(s)\mathrm{d}s\mathrm{d}t - V^{\mathrm{out}}(y^\star;\epsilon) + O(\epsilon) \tag{4.15}$$

with

$$V^{\mathrm{out}}(y^\star;\epsilon) = \frac{1}{4\pi}\int_{-\pi}^{\pi}\int_{0}^{\sqrt{\epsilon}} K_1(s,t)\left[\tilde{\mu}(s,t) - \tilde{\mu}(0,\cdot)\right] J(s,t)\sin(s)\mathrm{d}s\mathrm{d}t. \tag{4.16}$$

Note that $(s,t) \mapsto K_1(s,t)\left[\tilde{\mu}(s,t) - \tilde{\mu}(0,\cdot)\right] J(s,t)\sin(s)$ can be integrated, as a Cauchy principal value, allowing us to write (4.15) with (4.16). To determine the leading-order asymptotic behavior of $V^{\mathrm{out}}(y^\star;\epsilon)$, we proceed as in section 4.1. We substitute $s = \epsilon S$ into (4.16) and obtain

$$V^{\mathrm{out}}(y^\star;\epsilon) = \frac{1}{4\pi}\int_{-\pi}^{\pi}\int_{0}^{1/\sqrt{\epsilon}} K_1(\epsilon S,t)\left[\tilde{\mu}(\epsilon S,t) - \tilde{\mu}(0,\cdot)\right] J(\epsilon S,t)\sin(\epsilon S)\epsilon\mathrm{d}S\mathrm{d}t. \tag{4.17}$$

Recognizing that $\tilde{\nu}(\epsilon S,t) = \nu^\star + O(\epsilon)$ and $y_d(\epsilon S,t) = -\epsilon S y_s(0,\cdot) + O(\epsilon^2)$ with the vector $y_s(0,\cdot)$ lying on the plane tangent to B at $y^\star$, we find by expanding $K_1(\epsilon S,t)$ about $\epsilon = 0$ that

$$K_1(\epsilon S,t) = -\frac{\epsilon^{-3}\ell}{S^3|y_s(0,\cdot)|^3} + O(\epsilon^{-2}). \tag{4.18}$$

Since the leading-order behavior of K_1 is independent of t, we use (4.8) plus knowing that $J(\epsilon S, t) = J(0,\cdot) + O(\epsilon)$ and $\sin(\epsilon S) = \epsilon S + O(\epsilon^3)$ to obtain (see [19] for details)

$$\begin{aligned} V^{\text{out}}(y^\star;\epsilon) &= \frac{1}{4\pi}\int_0^\pi \int_0^{1/\sqrt{\epsilon}} \left[-\frac{\epsilon \ell J(0,\cdot)}{|y_s(0,\cdot)|^3}\tilde{\mu}_{ss}(0,\cdot) + O(\epsilon^2)\right] \mathrm{d}S\mathrm{d}t \\ &= -\frac{\sqrt{\epsilon}\ell J(0,\cdot)}{8|y_s(0,\cdot)|^3}\Delta_{S^2}\mu(y^\star) + O(\epsilon). \end{aligned} \tag{4.19}$$

Note that we have used (4.10) in the last step. Substituting this result into (4.15), we find that

$$\begin{aligned} U^{\text{out}}(y^\star;\epsilon,\delta) = \frac{1}{4\pi}\int_{-\pi}^{\pi}\int_0^\pi K_1(s,t)\left[\tilde{\mu}(s,t) - \tilde{\mu}(0,\cdot)\right] J(s,t)\sin(s)\mathrm{d}s\mathrm{d}t \\ + \sqrt{\epsilon}\frac{\ell J(0,\cdot)}{8|y_s(0,\cdot)|^3}\Delta_{S^2}\mu(y^\star) + O(\epsilon). \end{aligned} \tag{4.20}$$

This result gives the leading-order asymptotic behavior of U^{out}.

4.3. Three-dimensional asymptotic approximation. We obtain an asymptotic approximation for U by summing the leading-order behaviors obtained for U^{in} and U^{out} given in (4.12) and (4.20), respectively, which yields

$$\begin{aligned} U(y^\star;\epsilon) &= \frac{1}{4\pi}\int_{-\pi}^{\pi}\int_0^\pi K_1(s,t)\left[\tilde{\mu}(s,t) - \tilde{\mu}(0,\cdot)\right] J(s,t)\sin(s)\mathrm{d}s\mathrm{d}t + O(\epsilon) \\ &:= L_1[\mu] + O(\epsilon) \end{aligned} \tag{4.21}$$

with K_1 given in (4.18). It follows that the asymptotic approximation of $u(y^\star - \epsilon\ell\nu^\star)$ to $O(\epsilon^2)$ is given by

$$u(y^\star - \epsilon\ell\nu^\star) = f(y^\star) + \epsilon L_1[\mu] + O(\epsilon^2). \tag{4.22}$$

The structure of this asymptotic approximation for the close evaluation of the double-layer potential in three dimensions is exactly the same as what we found for the two-dimensional case: The leading-order asymptotic approximation is composed of the Dirichlet data and a nonlocal term coming from the outer expansion. Similarly, high-order asymptotic approximations could be obtained by continuing on to higher-order terms in the expansions U^{in} and U^{out}.

5. Numerical methods. We now use the results of the asymptotic analysis above to develop new numerical methods for the close evaluation problem. Numerical methods to compute the asymptotic approximations for the close evaluation of the double-layer potential must be sufficiently accurate in comparison to $O(\epsilon)$. Otherwise, the error made by the numerical method will dominate over the error of the asymptotic approximation. On the other hand, if the numerical method requires restrictively high resolution to compute the asymptotic approximation to sufficient accuracy, the numerical method suffers from the very issue of the close evaluation problem. In what follows, we describe numerical methods to compute the asymptotic approximations derived above at high accuracy with modest resolution requirements. From the computation of the asymptotic expansions, we found that splitting the integral into two parts ("close" to $y^\star$ and "far" from $y^\star$) was crucial for obtaining the leading-order behavior. We use the same integral splitting procedure in the numerical methods that follow.

5.1. Two dimensions. Suppose we have parameterized B by $y = y(\varphi)$ with $-\pi \leq \varphi \leq \pi$ with $y^\star = y(\varphi^\star)$. For that case, we need to compute

$$\mathscr{U}_1(y^\star) = \frac{1}{2\pi}\int_{-\pi}^{\pi} F_1(\varphi;\varphi^\star)\mathrm{d}\varphi \text{ with} \tag{5.1}$$

$$F_1(\varphi;\varphi^\star) = K_1(\varphi)J(\varphi)\left[\tilde{\mu}(\varphi) - \tilde{\mu}(\varphi^\star)\right], \tag{5.2}$$

where K_1 is given in (3.9). The function, K_1, is singular at $\varphi = \varphi^\star$. Consequently, applying a high-order accurate numerical quadrature rule to compute $\mathscr{U}_1$ will be limited in its accuracy even though F_1 vanishes identically at $\varphi = \varphi^\star$ due to the factor of $\tilde{\mu}(\varphi) - \tilde{\mu}(\varphi^\star)$. To improve the accuracy of a numerical evaluation of (5.1), we revisit the asymptotic expansion obtained for $V^{\text{out}}(y^\star;\epsilon)$ in (3.13)–(3.15). We split the integral according to

$$\mathscr{U}_1(y^\star) = \frac{1}{2\pi}\int_{-\pi}^{-\delta/2} F_1(\varphi;\varphi^\star)\mathrm{d}\varphi + \frac{1}{2\pi}\int_{\delta/2}^{\pi} F_1(\varphi;\varphi^\star)\mathrm{d}\varphi + \frac{1}{2\pi}\int_{-\delta/2}^{\delta/2} F_1(\varphi;\varphi^\star)\mathrm{d}\varphi,$$

where δ is a chosen constant (for numerical purposes, one can set δ to be the discretization step size). The last integral is analogous to $V^{\text{out}}(y^\star;\epsilon)$. Using the results from section 3.2, we find that

$$\frac{1}{2\pi}\int_{-\delta/2}^{\delta/2} F_1(\varphi;\varphi^\star)\mathrm{d}\varphi \sim -\frac{\delta}{4\pi}\frac{\ell\tilde{\mu}''(\varphi^\star)}{J(\varphi^\star)}, \quad \epsilon \to 0^+. \tag{5.3}$$

This result suggests the following method to compute $\mathscr{U}_1(y^\star)$ numerically using the N-point periodic trapezoid rule (PTR). Suppose we are given the grid function, $\tilde{\mu}(\varphi_j)$ for $j = 1,\ldots,N$ with $\varphi_j = -\pi + 2\pi(j-1)/N$, and suppose $\varphi^\star = \varphi_k$ is one of the quadrature points. We introduce the numerical approximation

$$\mathscr{U}_1(y^\star) \approx U_1^N(y^\star) = \frac{1}{N}\sum_{j\neq k} F_1(\varphi_j;\varphi_k) - \frac{\ell\tilde{\mu}''(\varphi_k)}{2NJ(\varphi_k)}, \tag{5.4}$$

where we have replaced the quadrature around $\varphi^\star$ with (5.3), and we have set $\delta = 2\pi/N$. We compute $\tilde{\mu}''(\varphi_k)$ with spectral accuracy using fast Fourier transform methods. Using this numerical approximation, we compute the $O(\epsilon^2)$ asymptotic approximation for the close evaluation of the double-layer potential in two dimensions through evaluation of

$$u(y^\star - \epsilon\ell\nu^\star) \approx f(y^\star) + \epsilon U_1^N(y^\star) + O(\epsilon^2). \tag{5.5}$$

To compute the $O(\epsilon^3)$ asymptotic approximation, in addition to $\mathscr{U}_1$, we need to compute

$$\mathscr{U}_2(y^\star) = \frac{1}{2\pi}\int_{-\pi}^{\pi} F_2(\varphi;\varphi^\star)\mathrm{d}\varphi, \tag{5.6}$$

where

$$F_2(\varphi;\varphi^\star) = K_2(\varphi)J(\varphi)\left[\tilde{\mu}(\varphi) - \tilde{\mu}(\varphi^\star)\right] \tag{5.7}$$

and K_2 given in (3.21). By using the higher-order asymptotic expansion for V^{out} (computed in the *Mathematica* notebook available on the GitHub repository [19]), we apply the same method used for $\mathscr{U}_1(y^\star)$ and arrive at

$$\mathscr{U}_2(y^\star) \approx U_2^N = \frac{1}{N}\sum_{j\neq k} F_2(\varphi_j;\varphi_k) - \frac{\ell^2\kappa^\star\tilde{\mu}''(\varphi_k)}{4NJ(\varphi_k)} \tag{5.8}$$

with $\kappa^\star$ denoting the signed curvature at $y^\star$. Using this numerical approximation, we compute the $O(\epsilon^3)$ asymptotic approximation for the close evaluation of the double-layer potential in two dimensions through evaluation of

$$u(y^\star - \epsilon\ell\nu^\star) \approx f(y^\star) + \epsilon U_1^N(y^\star) + \epsilon^2\left[U_2^N(y^\star) - \frac{\ell^2 y'(\varphi^\star)\cdot y''(\varphi^\star)}{4J^4(\varphi^\star)}\tilde{\mu}'(\varphi^\star) + \frac{\ell^2\tilde{\mu}''(\varphi^\star)}{4J^2(\varphi^\star)}\right] + O(\epsilon^3). \tag{5.9}$$

Since the boundary is given, we are able to compute $y'(\varphi)$ and $y''(\varphi)$ explicitly. We use fast Fourier transform methods to compute $\tilde{\mu}'(\varphi)$ and $\tilde{\mu}''(\varphi)$ with spectral accuracy.

The numerical method we propose (i) uses the asymptotic approximations as an alternative to a given quadrature rule (here PTR) when computing the solution for close evaluation points and (ii) takes advantage of the integral splitting method to determine corrections of the quadrature rule used to numerically compute the asymptotic approximations. In the numerical examples that follow, we will study the error made by the numerical evaluation of the asymptotic approximations with respect to ϵ, not with respect to N. Nonetheless, let us make some comments about how the integral splitting affects the quadrature rule (point (ii)). It has been shown that PTR has an exponential rate of convergence; however, for $\epsilon < 1/N$ one always encounters an $O(1)$ error [9]. By splitting the integral as we have done, we disrupt this spectral convergence for close evaluation points but maintain at least an $O(N^{-2})$ convergence rate with the trapezoid rule if the peaked behavior of the integrand is addressed. This is precisely what happens with (5.4)–(5.8). Further, one could consider applying the integral splitting method over multiple quadrature points, i.e., $\delta = j2\pi/N$ for some $j > 1$.

5.2. Three dimensions. Suppose we have parameterized B by $y = y(\theta, \varphi)$ with $\theta \in [0, \pi]$ and $\varphi \in [-\pi, \pi]$ with $y^\star = y(\theta^\star, \varphi^\star)$. For that case, we seek to compute

$$\mathscr{U}_1(y^\star) = \frac{1}{4\pi}\int_{-\pi}^{\pi}\int_0^{\pi} F_1(\theta, \varphi; \theta^\star, \varphi^\star)\sin(\theta)\mathrm{d}\theta\mathrm{d}\varphi \tag{5.10}$$

with

$$F_1(\theta, \varphi; \theta^\star, \varphi^\star) = K_1(\theta, \varphi)J(\theta, \varphi)\left[\tilde{\mu}(\theta, \varphi) - \tilde{\mu}(\theta^\star, \varphi^\star)\right], \tag{5.11}$$

where K_1 is given in (4.13). Just as with the two-dimensional case, the function K_1 is singular at $(\theta, \varphi) = (\theta^\star, \varphi^\star)$, so any attempt to apply a quadrature rule to compute $\mathscr{U}_1$ will be limited in its accuracy even though F_1 vanishes identically at $(\theta^\star, \varphi^\star)$ due to the factor of $\tilde{\mu}(\theta, \varphi) - \tilde{\mu}(\theta^\star, \varphi^\star)$.

To numerically evaluate (5.10), we apply a three-step method developed by the authors [18]. This method has been shown to be effective for computing layer potentials in three dimensions. We first rotate this integral to another spherical coordinate system in which $y^\star$ is aligned with the north pole (see Appendix B). This leads to $\theta = \theta(s, t)$ and $\varphi = \varphi(s, t)$ with $s \in [0, \pi]$ and $t \in [-\pi, \pi]$, where $\theta^\star = \theta(0, \cdot)$ and $\varphi^\star = \varphi(0, \cdot)$. We apply this rotation and find that

$$\mathscr{U}_1(y^\star) = \frac{1}{4\pi}\int_{-\pi}^{\pi}\int_0^{\pi} \tilde{F}(s, t)\sin(s)\mathrm{d}s\mathrm{d}t \tag{5.12}$$

with $\tilde{F}(s, t) = F_1(\theta(s, t), \varphi(s, t); \theta^\star, \varphi^\star)$. Now $\tilde{K}_1(\theta(s, t), \varphi(s, t))$ is singular at the north pole of this rotated coordinate system corresponding to $s = 0$. To improve

the accuracy of a numerical evaluation of (5.12), we revisit the asymptotic expansion obtained for $V^{\text{out}}(y^\star;\epsilon)$ in (4.19). By rewriting that result for the present context, we find that

$$\frac{1}{2}\int_0^\delta \left[\frac{1}{2\pi}\int_{-\pi}^{\pi} \tilde{F}(s,t)\mathrm{d}t\right]\sin(s)\mathrm{d}s = \int_0^\delta \left[-\frac{\ell J(0,\cdot)}{8|y_s(0,\cdot)|^3}\Delta_{S^2}\mu(y^\star)\right]\mathrm{d}s + O(\epsilon), \tag{5.13}$$

where δ is a chosen constant (for numerical purposes, one can set δ to be the discretization step size). Suppose we compute

$$\bar{F}(s) = \frac{1}{2\pi}\int_{-\pi}^{\pi} \tilde{F}(s,t)\mathrm{d}t. \tag{5.14}$$

The result in (5.13) suggests that $\bar{F}(s)$ smoothly limits to a finite value as $s \to 0$. Although we could use this result to evaluate $\bar{F}(s)$ in a numerical quadrature scheme, it will suffice to consider an open quadrature rule for s that does not include the point $s = 0$ such as the Gauss–Legendre quadrature. This result suggests the following three-step method to compute $\mathscr{U}_1(y^\star)$ numerically.

Let $t_k = -\pi + \pi(k-1)/N$ for $k = 1,\dots,2N$, and let z_j and w_j for $j = 1,\dots,N$ denote the N-point Gauss–Legendre quadrature abscissas and weights, respectively, such that

$$\int_{-1}^{1} f(x)\mathrm{d}x \approx \sum_{j=1}^{N} f(z_j)w_j. \tag{5.15}$$

We perform the mapping, $s_j = \pi(z_j+1)/2$ for $j = 1,\dots,N$, and make appropriate adjustments to the weights as shown below. For the first step, we rotate the spherical coordinate system so that $y^\star$ is aligned with its north pole as described in Appendix B. For the second step, we compute

$$\bar{F}(s_j) \approx \bar{F}_j^N = \frac{1}{2N}\sum_{k=1}^{2N} \tilde{F}(s_j,t_k), \quad j = 1,\dots,N. \tag{5.16}$$

For the third step, we compute the numerical approximation

$$\mathscr{U}_1(y^\star) \approx U_1^N(y^\star) = \frac{\pi}{4}\sum_{j=1}^{N} \bar{F}_j^N w_j. \tag{5.17}$$

In (5.17), a factor of $\pi/2$ is introduced to scale the quadrature weights due to the mapping from z_j to s_j, and a factor of $1/2$ remains from the factor of $1/4\pi$ in (5.10).

Using the numerical approximation U_1^N, we compute the $O(\epsilon^2)$ asymptotic approximation for the close evaluation of the double-layer potential in three dimensions through evaluation of

$$u(y^\star - \epsilon\ell\nu^\star) \approx f(y^\star) + \epsilon U_1^N(y^\star) + O(\epsilon^2). \tag{5.18}$$

The integral operator in the asymptotic approximation in three dimensions is better behaved than those in two dimensions. As a result, using an open quadrature rule for s circumvents the need to explicitly perform the integral splitting method. Nonetheless, the integral splitting method gives the insight needed to derive the three-step method described above. In the numerical examples that follow, we will study the error made by the numerical evaluation of the asymptotic approximation with respect to ϵ for close evaluation points, not with respect to N.

6. Numerical results. We present results that show the accuracy and efficiency of the numerical methods based on the asymptotic approximations for the close evaluation of the double-layer potential. For all of the examples shown, we prescribe Dirichlet data corresponding to a particular harmonic function. With those Dirichlet data, we solve the boundary integral equation (2.4) numerically to obtain the density, μ. We use that density to compute the double-layer potential using different methods for comparison. The results below show the error made in computing the harmonic function at close evaluation points. The MATLAB codes used to compute all of the following examples are available in a GitHub repository [19].

When the boundary integral equation for μ is resolved with limited resolution, standard numerical methods to compute the double-layer potential will inherit the error. How that error interacts with the error in the asymptotic approximation must then be considered. We will consider such an example for the three-dimensional case.

6.1. Two dimensions. For the two-dimensional examples, we use the harmonic function

$$u(x) = -\frac{1}{2\pi}\log|x - x_0| \tag{6.1}$$

with $x_0 \in \mathbb{R}^2 \setminus \bar{D}$ and prescribe Dirichlet data by evaluating this function on the boundary (the Dirichlet data are then $\mathcal{C}^\infty$). We solve the boundary integral equation (2.4) using the Nyström method with the N-point PTR resulting in the numerical approximation for the density, $\tilde{\mu}_j \approx \tilde{\mu}(\varphi_j)$ with $\varphi_j = -\pi + 2(j-1)\pi/N$ for $j = 1, \ldots, N$. We compute the close evaluation of the double-layer potential at points, $x = y^\star - \epsilon\nu^\star$ (from now on we set $\ell = 1$), using the following four methods:

1. *PTR method*—Compute the double-layer potential,

$$u(y^\star - \epsilon\nu^\star) = \frac{1}{2\pi}\int_{-\pi}^{\pi} \frac{\nu_y \cdot (y^\star - \epsilon\nu^\star - y)}{|y^\star - \epsilon\nu^\star - y|^2}\mu(y)\mathrm{d}\sigma_y,$$

using the same N-point PTR used to solve (2.4).

2. *Subtraction method*—Compute the modified double-layer potential,

$$u(y^\star - \epsilon\nu^\star) = -\mu(y^\star) + \frac{1}{2\pi}\int_{-\pi}^{\pi} \frac{\nu_y \cdot (y^\star - \epsilon\nu^\star - y)}{|y^\star - \epsilon\nu^\star - y|^2}\left[\mu(y) - \mu(y^\star)\right]\mathrm{d}\sigma_y,$$

using the same N-point PTR used to solve (2.4).

3. $O(\epsilon^2)$ *asymptotic approximation*—Compute the $O(\epsilon^2)$ asymptotic approximation given by (3.18) using the new numerical method given in (5.5) using the same N-point PTR used to solve (2.4).

4. $O(\epsilon^3)$ *asymptotic approximation*—Compute the $O(\epsilon^3)$ asymptotic approximation given by (3.22) using the new numerical method given in (5.9) using the same N-point PTR used to solve (2.4).

We consider two different domains, D:

- *A kite domain* whose boundary, B, is given by

$$y(t) = (\cos t + 0.65\cos 2t - 0.65, 1.5\sin t), \quad -\pi \le t \le \pi. \tag{6.2}$$

- *A star domain* whose boundary, B, is given by

$$y(t) = r(t)(\cos t, \sin t), \quad r(t) = 1 + 0.3\cos 5t, \quad -\pi \le t \le \pi. \tag{6.3}$$

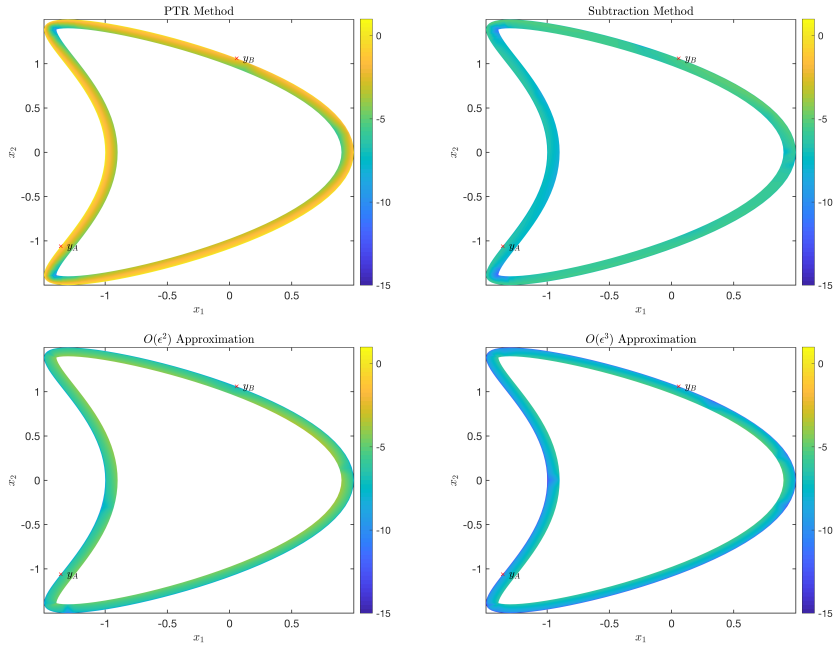

FIG. 3. *Plots of* $\log_{10}$ *of the error for the evaluation of the double-layer potential in the kite domain defined by* (6.2) *using four methods: the PTR method (upper left), the subtraction method (upper right), the* $O(\epsilon^2)$ *asymptotic approximation method (lower left), and the* $O(\epsilon^3)$ *asymptotic approximation method (lower right). In each of these plots, boundary points* $y_A = (-1.3571, -1.0607)$ *and* $y_B = (0.0571, 1.0607)$ *are plotted as red* $\times$*'s.*

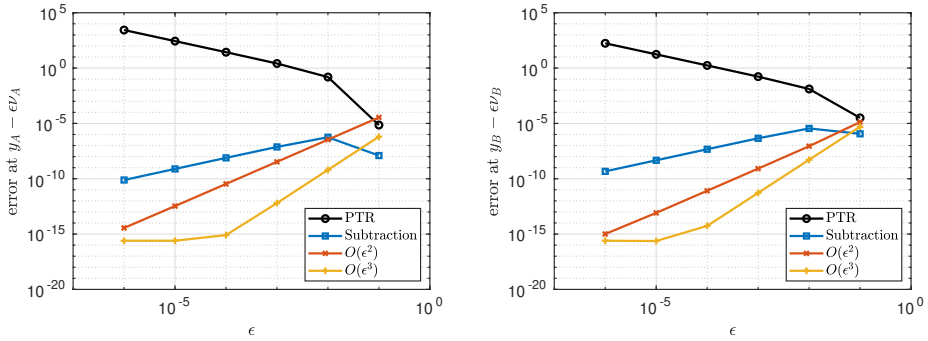

FIG. 4. *Log-log plots of the errors made in computing the double-layer potential by the four methods shown in Figure* 3 *at* $y_A - \epsilon\nu_A$ *(left) and at* $y_B - \epsilon\nu_B$ *(right) for* $10^{-6} \leq \epsilon \leq 10^{-1}$.

For both examples, we pick $x_0 = (1.85, 1.65)$, which lies outside the domains. We consider N fixed, $N = 128$, and study the dependence of the error on ϵ as $\epsilon \to 0^+$.

In Figure 3, we show results for the kite domain. The error, using a log scale, is presented for each of the four methods described above. The results show that the PTR method exhibits an $O(1)$ error as $\epsilon \to 0^+$. The subtraction method and the asymptotic approximations all show substantially smaller errors.

To compare the four methods more quantitatively, in Figure 4, we plot the errors made by the four methods at $y_A - \epsilon\nu_A$ (left) and $y_B - \epsilon\nu_B$ (right) with $10^{-6} \leq \epsilon \leq 10^{-1}$,

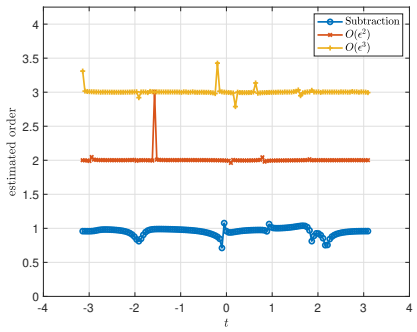

FIG. 5. *Estimated order of accuracy in computing the double-layer potential in the kite domain when using the subtraction method (blue ∘), the $O(\epsilon^2)$ asymptotic approximation method (red ×), and the $O(\epsilon^3)$ asymptotic approximation method (yellow +) for varying values of t.*

where ν_A and ν_B are the unit outward normals at $y_A = (-1.3571, -1.0607)$ and $y_B = (0.0571, 1.0607)$, respectively. The points y_A and y_B are shown in each plot of Figure 3. From the results in Figure 4, we observe that the error when using the PTR method increases as $\epsilon \to 0^+$, while the error in the other three methods decreases. The errors made by the asymptotic approximations are monotonically decreasing as $\epsilon \to 0^+$. However, the error made by the subtraction method presents a different behavior: It reaches a maximum at $\epsilon \approx 10^{-2}$, after which it decreases as ϵ increases. For larger values of ϵ, the double-layer potential is no longer nearly singular, so the N-point PTR (and therefore methods 1 and 2) become more accurate. The error is at a maximum for the subtraction method when $\epsilon = O(1/N)$, which is why we observe the maximum error occurring at $\epsilon \approx 10^{-2}$. The results in Figure 4 show a clear difference in the rate at which the errors vanish as $\epsilon \to 0^+$ between the subtraction method and the asymptotic approximation methods. The $O(\epsilon^3)$ asymptotic approximation decays the fastest, followed by the $O(\epsilon^2)$ asymptotic approximation and then the subtraction method. For $\epsilon < 10^{-4}$, the error incurred by the $O(\epsilon^3)$ asymptotic approximation levels out at machine precision. We estimate the rate at which the subtraction method and the asymptotic approximation methods decay with respect to ϵ from the slope of the best-fit line through the log-log plot of the error versus ϵ in Figure 5. We compute the slope for each evaluation point $y(t_j) - \epsilon\tilde{\nu}(t_j)$, where $t_j = -\pi + 2(j-1)\pi/N$ for $j = 1, \ldots, N$, and we vary ϵ. For the subtraction method, we consider ϵ values such that $10^{-6} \le \epsilon \le 10^{-2}$, and for the $O(\epsilon^2)$ and $O(\epsilon^3)$ asymptotic approximation methods, we consider the same range but only include values where the error is greater than 10^{-15}. The results shown in Figure 5 indicate that the subtraction method decays linearly with ϵ, and the rates of the asymptotic approximations are consistent with the analysis presented in section 3.

For the second example of computing the double-layer potential in the star domain, Figures 6–8 are analogous to Figures 3–5 for the kite domain. The characteristics of the errors for this second domain are exactly the same as described for the kite domain.

Summary of the results. In the case of two-dimensional problems, the subtraction method yields a method whose error decays linearly with the distance away from the boundary. The $O(\epsilon^2)$ and $O(\epsilon^3)$ asymptotic approximations methods are much more accurate for close evaluation points. Moreover, only relatively modest

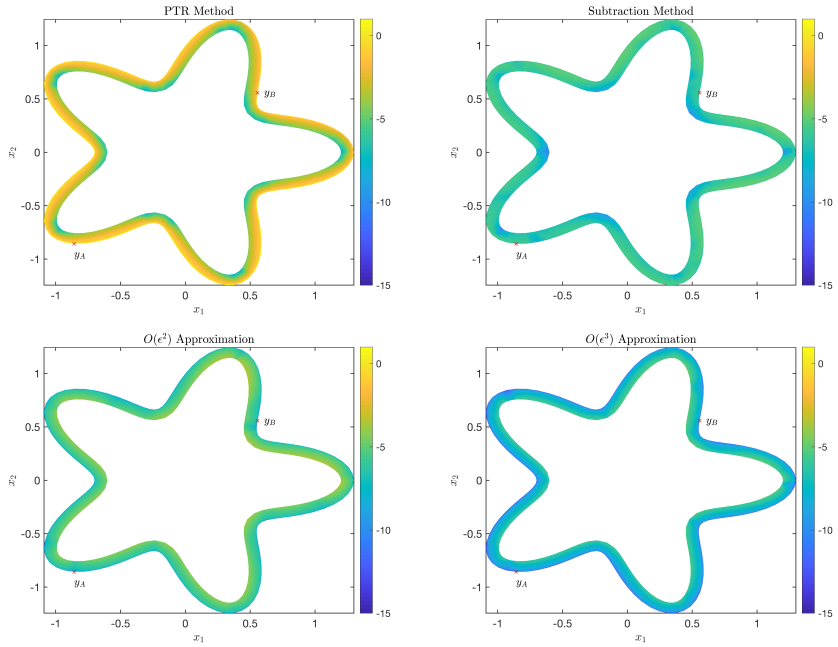

FIG. 6. *Plots of* $\log_{10}$ *of the error for the evaluation of the double-layer potential in the star domain defined by* (6.3) *using four methods: the PTR method (upper left), the subtraction method (upper right), the* $O(\epsilon^2)$ *asymptotic approximation method (lower left), and the* $O(\epsilon^3)$ *asymptotic approximation method (lower right). In each of these plots, boundary points* $y_A = (-1.3571, -1.0607)$ *and* $y_B = (0.0571, 1.0607)$ *are plotted as red* $\times$*'s.*

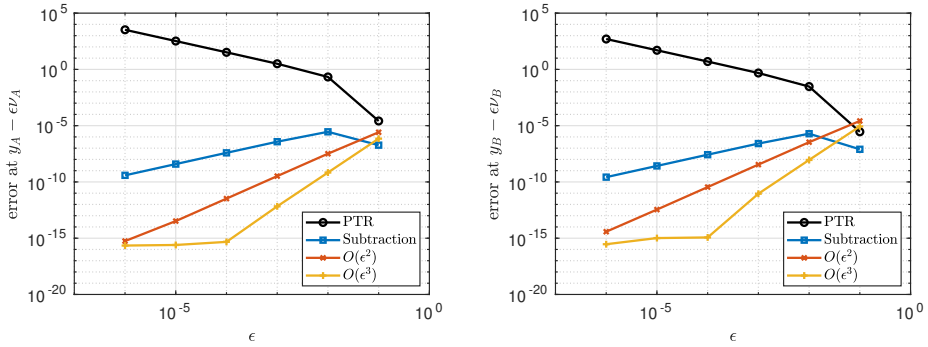

FIG. 7. *Log-log plots of the errors made in computing the double-layer potential by the four methods shown in Figure* 6 *at* $y_A - \epsilon\nu_A$ *(left) and at* $y_B - \epsilon\nu_B$ *(right) for* $10^{-6} \leq \epsilon \leq 10^{-1}$.

resolution is required for these asymptotic approximations to be effective. However, the errors for these asymptotic approximations are monotonically increasing with the distance to the boundary, so they are not accurate for points farther away from the boundary. The results given by the asymptotic analysis provide guidance on where to apply these asymptotic approximations effectively. For all of these reasons, we find that the asymptotic approximations and corresponding numerical methods are useful for two-dimensional problems.

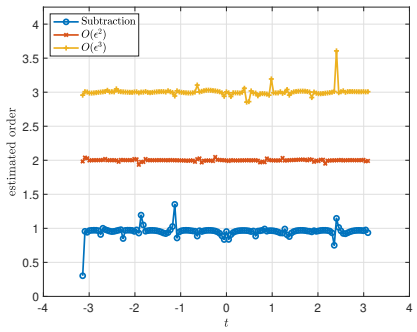

FIG. 8. *Estimated order of accuracy in computing the double-layer potential in the star domain when using the subtraction method (blue ∘), the $O(\epsilon^2)$ asymptotic approximation method (red ×), and the $O(\epsilon^3)$ asymptotic approximation method (yellow ∗) for varying values of t.*

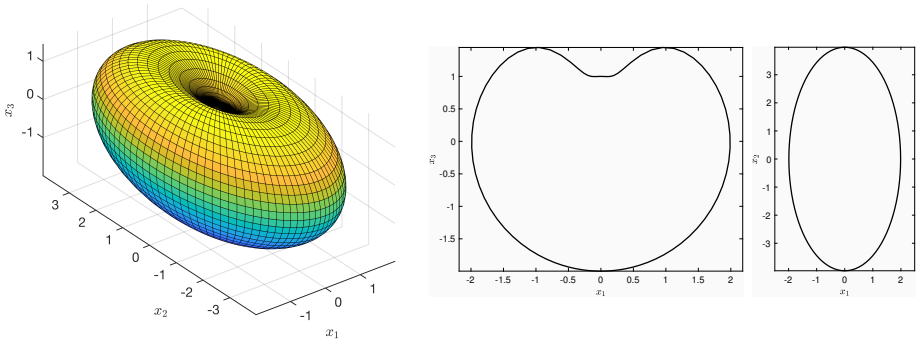

FIG. 9. *The boundary surface defined by* (6.5) *that is used to exemplify the evaluation of the double-layer potential in three dimensions (left) and the intersections of this boundary with the x_1x_3-plane (center) and x_1x_2-plane (right).*

6.2. Three dimensions. Let (x_1, x_2, x_3) denote an ordered triple in a Cartesian coordinate system. To study the computation of the double-layer potential in three dimensions, we consider the harmonic function

$$u(x_1, x_2, x_3) = \frac{1}{\sqrt{(x_1-5)^2 + (x_2-4)^2 + (x_3-3)^2}} \tag{6.4}$$

in the domain whose boundary is given by, for $\theta \in [0, \pi]$, $\varphi \in [-\pi, \pi]$,

$$y(\theta, \varphi) = \left[2 - \frac{1}{1 + 100(1-\cos\theta)^2}\right](\sin\theta\cos\varphi, 2\sin\theta\sin\varphi, \cos\theta). \tag{6.5}$$

This boundary surface is shown in Figure 9 (left) along with its intersection with the vertical x_1x_3-plane (center) and the horizontal x_1x_2-plane (right). We solve boundary integral equation (2.4) using the Galerkin method [4, 5, 6, 7]. The Galerkin method approximates the density according to

$$\tilde{\mu}(\theta, \varphi) \approx \tilde{\mu}^N(\theta, \varphi) = \sum_{n=0}^{N-1} \sum_{m=-n}^{n} \hat{\mu}_{nm} Y_{nm}(\theta, \varphi) \tag{6.6}$$

with $\{Y_{nm}\}$ denoting the orthonormal set of spherical harmonics. For these results, we

have set $N = 48$. We have computed the close evaluation of the double-layer potential at points $x = y^\star - \epsilon\nu^\star$, using the following two different methods for comparison.

1. *Numerical approximation*—Compute the modified double-layer potential,

$$u(y^\star - \epsilon\nu^\star) = -\mu(y^\star) + \frac{1}{4\pi}\int_B \frac{\nu_y \cdot (y^\star - \epsilon\nu^\star - y)}{|y^\star - \epsilon\nu^\star - y|^3}\,[\mu(y) - \mu(y^\star)]\,\mathrm{d}\sigma_y,$$

using the three-step numerical method described in [18]. For the first step, the modified double-layer potential is written in spherical coordinates that have been rotated so that $y^\star$ is aligned with the north pole. For the second step, the $2N$-point PTR is used to compute the integral in the azimuthal angle. For the third step, the N-point Gauss–Legendre quadrature rule mapped to $[0, \pi]$ is used to compute the integral in the polar angle.

2. $O(\epsilon^2)$ *Asymptotic approximation*—Compute the asymptotic approximation given by (4.22) using the method given in (5.18) (with $N = 48$).

The error of the numerical method has been shown to decay quadratically with ϵ when $\epsilon \ll 1/N$ [18]. This quadratic error decay occurs because, in the rotated coordinate system, the azimuthal integration acts as an averaging operation yielding a smooth function of the polar angle that is computed to high order using Gaussian quadrature. However, this asymptotic error estimate is valid only when the numerical approximation of the density is sufficiently resolved. If N in (6.6) is not sufficiently large that $|\hat{\mu}_{nm}|$ for $n > N$ is negligibly small, then the truncation error associated with (6.6) may interrupt this quadratic error decay. For the domain here, with $N = 48$, we find that the estimated truncation error for (6.6) is approximately 10^{-8}. While this error is relatively small, it is not small enough to observe the error's quadratic rate of decay. We would have to consider a much larger value of N to observe that decay rate. However, computing the numerical solution of boundary integral equation (2.4) with $N > 48$ becomes restrictively large. For this case, a question emerges about how well the asymptotic approximations perform when one has limited resolution for the density. In what follows, we evaluate what the subtraction method and the $O(\epsilon^2)$ asymptotic approximation method do in this limited resolution situation.

Error results for the computation of the double-layer potential in this domain for each of the two methods described above appear in Figure 10. The top row shows the error on the slice of the domain through the vertical x_1x_3-plane for the numerical method (left) and the $O(\epsilon^2)$ asymptotic approximation method (right). The point $y_A = (1.7830, 0, 0.8390)$ is plotted as a red $\times$ symbol in both plots. The bottom row shows the errors of the same methods (left for the numerical method, right for the $O(\epsilon^2)$ asymptotic approximation method) on the slice of the domain through the horizontal x_1x_2-plane. The point $y_B = (1.7439, 1.19175, 0)$ is plotted as a red $\times$ symbol in both plots.

In Figure 11, we show the errors computed at $y_A - \epsilon\nu_A$ (left) and $y_B - \epsilon\nu_B$ (right) for varying ϵ, where ν_A and ν_B are the unit outward normals at y_A and y_B, respectively. In contrast to the two-dimensional results, we find that the error for the numerical method is approximately 10^{-8} for all values of ϵ. This error is due to the truncation error made by the Galerkin method. Because the truncation error dominates at this resolution, we are not able to see its quadratic decay as $\epsilon \to 0^+$. If a higher-resolution computation were used to solve the boundary integral equation, the error of the numerical method would exhibit a similar behavior to that made by the subtraction method for the two-dimensional examples. In particular, the error would have a maximum at $\epsilon = O(1/N)$ about which the error decays. We observe that the $O(\epsilon^2)$ asymptotic method decays monotonically with ϵ even when $N = 48$.

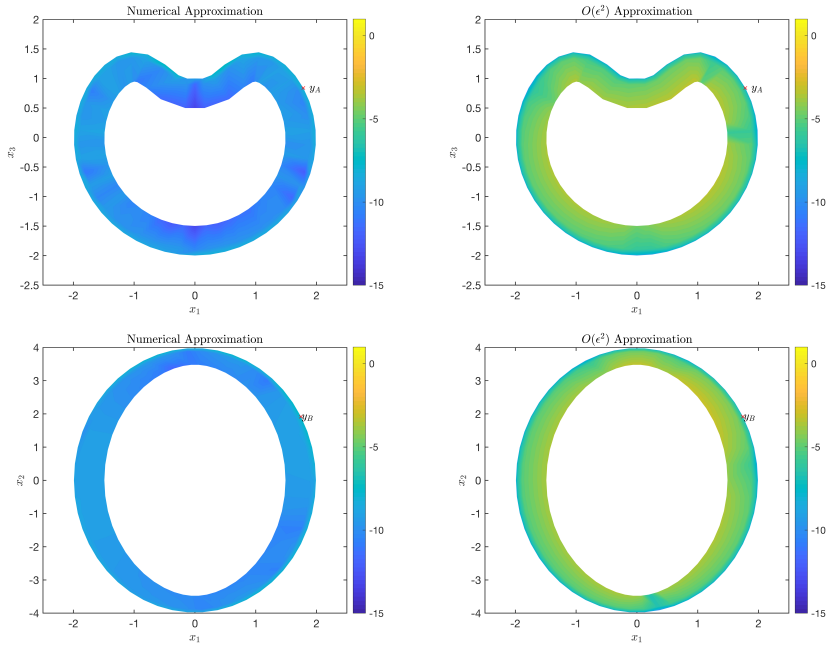

FIG. 10. *Plots of* $\log_{10}$ *of the error made in computing the double-layer potential by the numerical approximation (left column) and the* $O(\epsilon^2)$ *asymptotic approximation (right column) in the domain whose boundary is shown in Figure* 9. *The top row of plots show the error on the* x_1x_3*-plane, and the bottom row of plots show the error on the* x_1x_2*-plane. In the top row of plots, the point* $y_A = (1.7830, 0, 0.8390)$ *is plotted as a red* $\times$*, and in the bottom row of plots, the point* $y_B = (1.7439, 1.19175, 0)$ *is plotted as a red* $\times$.

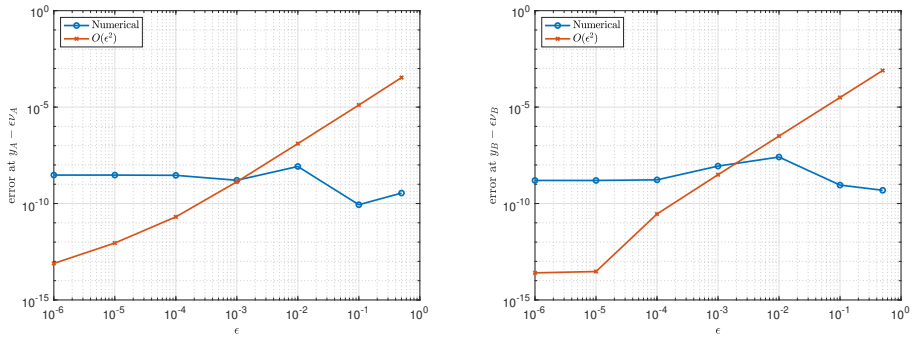

FIG. 11. *Log-log plots of the errors made by the two methods shown in Figure* 10 *at* $y_A - \epsilon\nu_A$ *(left) and at* $y_B - \epsilon\nu_B$ *(right) for* $10^{-6} \leq \epsilon \leq 0.5$.

We estimate the order of accuracy in Figure 12. The results for the estimated order of accuracy over the points intersecting the vertical x_1x_3-plane are shown in the left plot of Figure 12. For those results, we determine the estimated order of accuracy by determining the best-fit line through the log-log plot of the error versus ϵ for several values of the extended polar angle, $s_0 \in [0, 2\pi]$. This extended polar angle parameterizes the circle on the unit sphere lying on the x_1x_3-plane that starts and ends at the north pole. The results for the estimated order of accuracy over the points intersecting the horizontal x_1x_2-plane are shown in the right plot of Figure 12. For

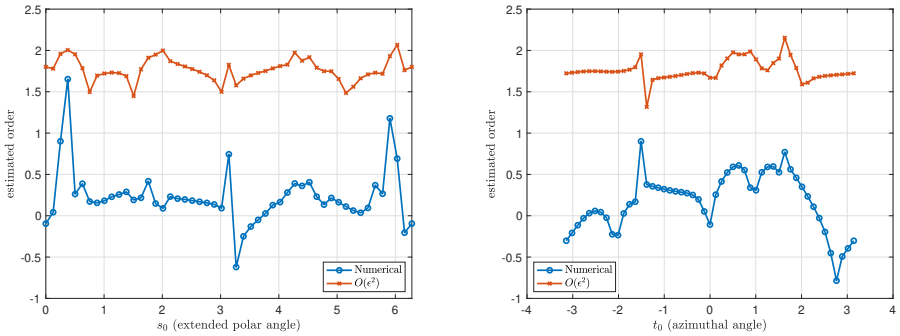

FIG. 12. *Estimated order of accuracy for the numerical approximation (blue ∘) and the $O(\epsilon^2)$ asymptotic approximation (red ×) on the x_1x_3-plane (left plot) and on the x_1x_2-plane (right plot). Results on the x_1x_3-plane are given in terms of the extended polar angle, $s_0 \in [0, 2\pi]$, which parameterizes the circle on the unit sphere lying on the x_1x_3-plane that starts and ends at the north pole. Results on the x_1x_2-plane are given in terms of the azimuthal angle, $t_0 \in [0, 2\pi]$.*

those results, we determine the estimated order of accuracy by determining the best-fit line through the log-log plot of the error versus ϵ for several values of the azimuthal angle, $t_0 \in [0, 2\pi]$. Because of the resolution limitation in the Galerkin method, we are not able to see that the order of accuracy for the numerical method is two. In fact, the error is nearly uniform with respect to ϵ because it is the truncation error of (6.6) that is dominating. Despite the resolution limitation in the Galerkin method, we find that the $O(\epsilon^2)$ asymptotic approximation has an order accuracy of nearly two. These results suggest that the asymptotic approximation offers an effective alternative when the resolution of the boundary integral equation is limited.

Summary of the results. For three-dimensional problems, the subtraction method is more effective when computed in an appropriate rotated coordinate system than for two-dimensional problems. The subtraction method is more effective in three dimensions because in this rotated coordinate system, integration with respect to the azimuthal angle is a natural averaging operation that regularizes the integral, thereby allowing for the use of a high-order quadrature rules for integration with respect to the polar angle. Provided that the density is sufficiently resolved, the subtraction method has been shown to decay quadratically with the distance away from the boundary [18]. The $O(\epsilon^2)$ asymptotic approximation also decays quadratically. However, it is not as sensitive to the accuracy of the density. For this reason, we find that the asymptotic approximation is a good alternative for three-dimensional problems, especially when the density is not highly resolved.

7. Conclusion. We have evaluated the leading-order asymptotic behavior for the close evaluation of the double-layer potential in two and three dimensions. By developing new numerical methods using these asymptotic approximations, we obtain accurate and effective methods for computing double-layer potentials at close evaluation points. Our numerical examples demonstrate the effectiveness of these asymptotic approximations and corresponding numerical methods.

The key to this methodology of using the asymptotic analysis is the insight it provides. The leading-order asymptotic behavior of the close evaluation of the double-layer potential is given by its local Dirichlet data plus a correction that is nonlocal. It is this nonlocal term that makes the close evaluation problem challenging to address

using only numerical methods. It is consistent with the fact that solutions of boundary value problems for elliptic partial differential equations have a global dependence on their boundary data. By explicitly computing this correction using asymptotic analysis, we have been able to develop an effective numerical method for the close evaluation problem. Moreover, the asymptotic error estimates provide guidance on where to apply these approximations, namely, for evaluation points closer to the boundary than the boundary mesh spacing. The result of this work is an accurate and efficient method for computing the close evaluation of the double-layer potential.

Future work includes rigorously proving the assumptions we have made in the asymptotic analysis conjectures. Then, the asymptotic approximation method can be extended to other layer potentials and other boundary value problems. Future work will include extending these methods to applications of Stokes flow, plasmonics, and others.

Appendix A. Uniform bounds for nonuniform asymptotic expansions. In this section we provide justification for the order of the asymptotic expansions after integration for (3.8), (3.15), (4.12), and (4.19). Throughout the paper, we assume that the general boundary B is an analytic closed boundary that can be mapped to S^{n-1}, $n = 2, 3$ (with an analytic diffeomorphism). Therefore, we establish the result for the unit circle (where calculations are explicit) and for the integrand of (3.5). To obtain (3.15), (4.12), and (4.19) one proceeds similarly. One can check that in this case the integrand of (3.5) becomes

$$F(t;\epsilon) = \frac{\ell(\epsilon\ell - 2)}{2} \frac{1}{2 + \epsilon\ell(\epsilon\ell - 2) + 2(\epsilon\ell - 1)\cos(t)} (\mu(t) - \mu(0)) \tag{A.1}$$

with the abuse of notation $\mu(t) = \mu(y(t))$.

LEMMA A.1 (nonuniform expansion with uniform bounds on the unit circle).

$$\int_{-\sqrt{\epsilon}}^{\sqrt{\epsilon}} F(t;\epsilon)dt = \int_{-1/\sqrt{\epsilon}}^{1/\sqrt{\epsilon}} \epsilon F(\epsilon T;\epsilon)dT = \sum_{k=0}^{N} \epsilon^k a_k + O(\epsilon^N)$$

for F given by (A.1) *with $(a_k)_k$ depending on μ and its derivatives at* 0.

Proof. The proof is divided into three steps.

Step 1: *Write $F(\epsilon T;\epsilon) = \sum_{k=-1}^{N} \epsilon^k F_k(T) + O(\epsilon^{N+1})$, and provide an explicit expression for $F_k(T)$.* We define $G(t;\epsilon) := 2 + \epsilon\ell(\epsilon\ell - 2) + 2(\epsilon\ell - 1)\cos(t)$. By substituting $t = \epsilon T$ and expanding about $\epsilon = 0$, we get

$$\begin{aligned} G(\epsilon T;\epsilon) &= 2 + \epsilon^2\ell^2 - 2\epsilon\ell + 2(\epsilon\ell - 1)\left[1 - \frac{\epsilon^2 T^2}{2} + \frac{\epsilon^4 T^4}{4!} + \cdots\right], \\ &= \epsilon^2(\ell^2 + T^2)\left[1 - \epsilon\frac{\ell T^2}{\ell^2 + T^2} + \epsilon^2 P(\epsilon, T)\right], \end{aligned}$$

where $P(\epsilon, T)$ is a polynomial in ϵ and a sum of rational functions in T. Then, after expanding and rearranging the terms, we have

$$\begin{aligned} \frac{1}{G(\epsilon T;\epsilon)} &= \frac{1}{\epsilon^2(\ell^2 + T^2)}\left[1 + \sum_{m=1}^{N}\left[-\epsilon\frac{\ell T^2}{\ell^2 + T^2} + \epsilon^2 P(\epsilon, T)\right]^m\right], \\ &= \frac{1}{\epsilon^2}\frac{1}{(\ell^2 + T^2)} + \sum_{m=-1}^{N-2} \epsilon^m P_m(T) + \cdots \end{aligned}$$

where

$$P_m(T) = \frac{\sum_{j=m+1}^{2m+4} \alpha_j T^j}{(\ell^2+T^2)^{m+3}}$$

with $\alpha_j \in \mathbb{R}$, $j \in \mathbb{N}$ polynomial coefficients. From here on, we will still denote α_j while the value can change after each operation. Plugging this expansion into F and expanding the density, $\mu(t)$, we obtain, again after combining terms,

$$\begin{aligned} F(\epsilon T;\epsilon) &= \frac{\ell(\epsilon\ell-2)}{2}\left[\frac{1}{\epsilon^2}\frac{1}{(\ell^2+T^2)} + \sum_{m=-1}^{N-2}\epsilon^m P_m(T) + \cdots\right]\left[\sum_{k=1}^{N}\epsilon^k T^k \mu^{(k)}(0) + \cdots\right] \\ &= -\frac{\ell T\mu'(0)}{\epsilon(\ell^2+T^2)} + \sum_{k=0}^{N}\epsilon^k F_k(T) + O(\epsilon^{N+1}) = \sum_{k=-1}^{N}\epsilon^k F_k(T) + O(\epsilon^{N+1}) \end{aligned}$$

with

$$F_k(T) = \frac{\sum_{j=k+1}^{3(k+1)} \alpha_j(\mu) T^j}{(\ell^2+T^2)^{k+2}},$$

$k \geq 2$, and $\alpha_j(\mu) \in \mathbb{R}$ coefficients depending on μ and its derivatives at 0. F_0 and F_1 can be found in the *Mathematica* notebook [19].

Step 2: *Prove that* $\int_{-1/\sqrt{\epsilon}}^{1/\sqrt{\epsilon}} \epsilon^{k+1} F_k(T)dT = O(\epsilon^k)$ *for all* $k \geq 0$. One can check that $\int_{-1/\sqrt{\epsilon}}^{1/\sqrt{\epsilon}} F_{-1}(T)dT = 0$, and a straightforward computation gives that $\int_{-1/\sqrt{\epsilon}}^{1/\sqrt{\epsilon}} \epsilon^{k+1} F_k(T)dT = O(\epsilon^k)$, $k = 0, 1$. Details of calculations can be found in the *Mathematica* notebook [19]. Note that some of the integrals are treated as a Cauchy principal value. For $k \geq 2$, one has

$$|F_k(T)| \leq \sum_{j=k+1}^{3(k+1)} |\alpha_j(\mu)| T^{j-2k-4} \leq \sum_{j=-k-3}^{k-1} |\alpha_j(\mu)| T^j.$$

It follows that

$$\left|\int_{-1/\sqrt{\epsilon}}^{1/\sqrt{\epsilon}} \epsilon^{k+1} F_k(T)dT\right| \leq \sum_{j=1}^{2k+3} |\alpha_j(\mu)| \epsilon^{\frac{2k+1-j}{2}} \leq M_k \epsilon^k,\ M_k = 2(k+1) \max_{j\in[\![1,2k+3]\!]} |\alpha_j(\mu)|,$$

leading to

$$\int_{-1/\sqrt{\epsilon}}^{1/\sqrt{\epsilon}} \epsilon^{k+1} F_k(T)dT = O(\epsilon^k) \text{ for all } k \geq 0.$$

Step 3: *Establish uniform convergence.* We have

$$\int_{-\sqrt{\epsilon}}^{\sqrt{\epsilon}} F(t;\epsilon)dt = \int_{-1/\sqrt{\epsilon}}^{1/\sqrt{\epsilon}} \epsilon F(\epsilon T;\epsilon)dT = \int_{-1/\sqrt{\epsilon}}^{1/\sqrt{\epsilon}} \left(\sum_{k=0}^{N} \epsilon^{k+1} F^k(T) + O(\epsilon^{N+2})\right) dT.$$

Using Tonelli's theorem, it follows that

$$\begin{aligned} &\left|\int_{-1/\sqrt{\epsilon}}^{1/\sqrt{\epsilon}} \epsilon F(\epsilon T;\epsilon) - \sum_{k=0}^{N} \epsilon^{k+1} F^k(T)dT\right| = \left|\int_{-1/\sqrt{\epsilon}}^{1/\sqrt{\epsilon}} \left(\sum_{k=N+1}^{\infty} \epsilon^{k+1} F^k(T)\right) dT\right|, \\ &\leq \sum_{k=N+1}^{\infty} \left|\int_{-1/\sqrt{\epsilon}}^{1/\sqrt{\epsilon}} \epsilon^{k+1} F^k(T)dT\right| \leq \sum_{k=N+1}^{\infty} M_k \epsilon^k \leq M_{N+1}\epsilon^{N+1}\left(1 + \sum_{k=1}^{\infty} \tilde{M}_k \epsilon^k\right), \end{aligned}$$

leading to

$$\int_{-1/\sqrt{\epsilon}}^{1/\sqrt{\epsilon}} \left(\epsilon F(\epsilon T; \epsilon) - \sum_{k=0}^{N} \epsilon^{k+1} F^k(T) \right) dT = O(\epsilon^{N+1}). \qquad \square$$

Appendix B. Rotations on the sphere. We give the explicit rotation formulas over the sphere used in the numerical method for the asymptotic approximation in three dimensions. Consider $y, y^\star \in S^2$. We introduce the parameters $\theta \in [0, \pi]$ and $\varphi \in [-\pi, \pi]$ and write

$$y = y(\theta, \varphi) = \sin\theta\cos\varphi\,\hat{\imath} + \sin\theta\sin\varphi\,\hat{\jmath} + \cos\theta\,\hat{k}. \tag{B.1}$$

The parameter values, $\theta^\star$ and $\varphi^\star$, are set such that $y^\star = y(\theta^\star, \varphi^\star)$. We would like to work in the rotated, uvw-coordinate system in which

$$\begin{aligned} \hat{u} &= \cos\theta^\star\cos\varphi^\star\,\hat{\imath} + \cos\theta^\star\sin\varphi^\star\,\hat{\jmath} - \sin\theta^\star\,\hat{k}, \\ \hat{v} &= -\sin\varphi^\star\,\hat{\imath} + \cos\varphi^\star\,\hat{\jmath}, \\ \hat{w} &= \sin\theta^\star\cos\varphi^\star\,\hat{\imath} + \sin\theta^\star\sin\varphi^\star\,\hat{\jmath} + \cos\theta^\star\,\hat{k}. \end{aligned} \tag{B.2}$$

Notice that $\hat{w} = y^\star$. For this rotated coordinate system, we introduce the parameters $s \in [0, \pi]$ and $t \in [-\pi, \pi]$ such that

$$y = y(s, t) = \sin s\cos t\,\hat{u} + \sin s\sin t\,\hat{v} + \cos s\,\hat{w}. \tag{B.3}$$

It follows that $y^\star = y(0, \cdot)$. By equating (B.1) and (B.3) and substituting (B.2) into that result, we obtain

$$\begin{bmatrix} \sin\theta\cos\varphi \\ \sin\theta\sin\varphi \\ \cos\theta \end{bmatrix} = \begin{bmatrix} \cos\theta^\star\cos\varphi^\star & -\sin\varphi^\star & \sin\theta^\star\cos\varphi^\star \\ \cos\theta^\star\sin\varphi^\star & \cos\varphi^\star & \sin\theta^\star\sin\varphi^\star \\ -\sin\theta^\star & 0 & \cos\theta^\star \end{bmatrix} \begin{bmatrix} \sin s\cos t \\ \sin s\sin t \\ \cos s \end{bmatrix}. \tag{B.4}$$

We rewrite (B.4) compactly as $\hat{y}(\theta, \varphi) = R(\theta^\star, \varphi^\star)\hat{y}(s, t)$ with $R(\theta^\star, \varphi^\star)$ denoting the 3×3 orthogonal rotation matrix. We now seek to write $\theta = \theta(s, t)$ and $\varphi = \varphi(s, t)$. To do so, we introduce

$$\xi(s, t; \theta^\star, \varphi^\star) = \cos\theta^\star\cos\varphi^\star\sin s\cos t - \sin\varphi^\star\sin s\sin t + \sin\theta^\star\cos\varphi^\star\cos s, \tag{B.5}$$

$$\eta(s, t, \theta^\star, \varphi^\star) = \cos\theta^\star\sin\varphi^\star\sin s\cos t + \cos\varphi^\star\sin s\sin t + \sin\theta^\star\sin\varphi^\star\cos s, \tag{B.6}$$

$$\zeta(s, t, \theta^\star, \varphi^\star) = -\sin\theta^\star\sin s\cos t + \cos\theta^\star\cos s. \tag{B.7}$$

From (B.4), we find that

$$\theta = \arctan\left(\frac{\sqrt{\xi^2 + \eta^2}}{\zeta} \right) \text{ and } \varphi = \arctan\left(\frac{\eta}{\xi} \right). \tag{B.8}$$

With these formulas, we can write $\theta = \theta(s, t)$ and $\varphi = \varphi(s, t)$.

Appendix C. Spherical Laplacian. In this appendix, we establish the result given in (4.10). We first seek an expression for $\partial_s^2[\cdot]|_{s=0}$ in terms of θ and φ. By the chain rule, we find that

$$\frac{\partial^2}{\partial s^2}[\cdot]\Big|_{s=0} = \left[\left(\frac{\partial\theta}{\partial s} \right)^2 \frac{\partial^2}{\partial\theta^2} + \left(\frac{\partial\varphi}{\partial s} \right)^2 \frac{\partial^2}{\partial\varphi^2} + 2\frac{\partial\theta}{\partial s}\frac{\partial\varphi}{\partial s}\frac{\partial^2}{\partial\theta\partial\varphi} + \frac{\partial^2\theta}{\partial s^2}\frac{\partial}{\partial\theta} + \frac{\partial^2\varphi}{\partial s^2}\frac{\partial}{\partial\varphi} \right] \Big|_{s=0}. \tag{C.1}$$

Using θ and φ defined in (B.8), we find that

$$\left.\frac{\partial\theta(s,t)}{\partial s}\right|_{s=0} = \cos t, \quad \left.\frac{\partial^2\theta(s,t)}{\partial s^2}\right|_{s=0} = \frac{\cos\theta^\star}{\sin\theta^\star}\sin^2 t, \tag{C.2}$$

$$\left.\frac{\partial\varphi(s,t)}{\partial s}\right|_{s=0} = \frac{\sin t}{\sin\theta^\star}, \quad \left.\frac{\partial^2\varphi(s,t)}{\partial s^2}\right|_{s=0} = -\frac{\cos\theta^\star}{\sin^2\theta^\star}\sin 2t. \tag{C.3}$$

Note that at $s=0$, we have $\theta^\star = \theta$. Substituting (C.2)–(C.3) into (C.1) and replacing $\theta^\star$ by θ, we obtain

$$\begin{aligned}\left.\frac{\partial^2}{\partial s^2}[\cdot]\right|_{s=0} = \cos^2 t\frac{\partial^2}{\partial\theta^2} + \sin^2 t\frac{1}{\sin^2\theta}\frac{\partial^2}{\partial\varphi^2} + 2\cos t\sin t\frac{1}{\sin\theta}\frac{\partial^2}{\partial\theta\partial\varphi} \\ + \sin^2 t\frac{\cos\theta}{\sin\theta}\frac{\partial}{\partial\theta} - \sin 2t\frac{\cos\theta}{\sin^2\theta}\frac{\partial}{\partial\varphi},\end{aligned} \tag{C.4}$$

from which it follows that

$$\frac{1}{\pi}\int_0^\pi \left.\frac{\partial^2}{\partial s^2}[\cdot]\right|_{s=0} \mathrm{d}t = \frac{1}{2}\left[\frac{\partial^2}{\partial\theta^2} + \frac{\cos\theta}{\sin\theta}\frac{\partial}{\partial\theta} + \frac{1}{\sin^2\theta}\frac{\partial^2}{\partial\varphi^2}\right] = \frac{1}{2}\Delta_{S^2}, \tag{C.5}$$

which establishes the result.

REFERENCES

[1] L. af Klinteberg and A.-K. Tornberg, *A fast integral equation method for solid particles in viscous flow using quadrature by expansion*, J. Comput. Phys., 326 (2016), pp. 420–445.

[2] L. af Klinteberg and A.-K. Tornberg, *Error estimation for quadrature by expansion in layer potential evaluation*, Adv. Comput. Math., 43 (2017), pp. 195–234.

[3] G. M. Akselrod, C. Argyropoulos, T. B. Hoang, C. Ciracì, C. Fang, J. Huang, D. R. Smith, and M. H. Mikkelsen, *Probing the mechanisms of large Purcell enhancement in plasmonic nanoantennas*, Nat. Photonics, 8 (2014), pp. 835–840.

[4] K. E. Atkinson, *The numerical solution Laplace's equation in three dimensions*, SIAM J. Numer. Anal., 19 (1982), pp. 263–274.

[5] K. E. Atkinson, *Algorithm* 629: *An integral equation program for Laplace's equation in three dimensions*, ACM Trans. Math. Software, 11 (1985), pp. 85–96.

[6] K. E. Atkinson, *A survey of boundary integral equation methods for the numerical solution of Laplace's equation in three dimensions*, in Numerical Solution of Integral Equations, Springer, New York, 1990, pp. 1–34.

[7] K. E. Atkinson, *The Numerical Solution of Integral Equations of the Second Kind*, Cambridge University Press, Cambridge, 1997.

[8] A. Barnett, B. Wu, and S. Veerapaneni, *Spectrally accurate quadratures for evaluation of layer potentials close to the boundary for the* 2*d Stokes and Laplace equations*, SIAM J. Sci. Comput., 37 (2015), pp. B519–B542.

[9] A. H. Barnett, *Evaluation of layer potentials close to the boundary for Laplace and Helmholtz problems on analytic planar domains*, SIAM J. Sci. Comput., 36 (2014), pp. A427–A451.

[10] J. T. Beale and M.-C. Lai, *A method for computing nearly singular integrals*, SIAM J. Numer. Anal., 38 (2001), pp. 1902–1925.

[11] J. T. Beale, W. Ying, and J. R. Wilson, *A simple method for computing singular or nearly singular integrals on closed surfaces*, Commun. Comput. Phys., 20 (2016), pp. 733–753.

[12] C. Carvalho, S. Khatri, and A. D. Kim, *Asymptotic analysis for close evaluation of layer potentials*, J. Comput. Phys., 355 (2018), pp. 327–341.

[13] C. L. Epstein, L. Greengard, and A. Klöckner, *On the convergence of local expansions of layer potentials*, SIAM J. Numer. Anal., 51 (2013), pp. 2660–2679.

[14] R. B. Guenther and J. W. Lee, *Partial Differential Equations of Mathematical Physics and Integral Equations*, Dover, New York, 1996.

[15] J. Helsing and R. Ojala, *On the evaluation of layer potentials close to their sources*, J. Comput. Phys., 227 (2008), pp. 2899–2921.

[16] E. J. Hinch, *Perturbation Methods*, Cambridge University Press, Cambridge, 1991.
[17] E. E. Keaveny and M. J. Shelley, *Applying a second-kind boundary integral equation for surface tractions in Stokes flow*, J. Comput. Phys., 230 (2011), pp. 2141–2159.
[18] S. Khatri, A. D. Kim, R. Cortez, and C. Carvalho, *Close Evaluations of Layer Potentials in Three Dimensions*, arXiv:1807.02474, 2019.
[19] A. D. Kim, *Asymptotic-DLP*, https://github.com/arnolddkim/Asymptotic-DLP, 2018.
[20] A. Klöckner, A. Barnett, L. Greengard, and M. O'Neil, *Quadrature by expansion: A new method for the evaluation of layer potentials*, J. Comput. Phys., 252 (2013), pp. 332–349.
[21] R. Kress, *Linear Integral Equations*, Springer, New York, 1999.
[22] S. A. Maier, *Plasmonics: Fundamentals and Applications*, Springer, New York, 2007.
[23] G. R. Marple, A. Barnett, A. Gillman, and S. Veerapaneni, *A fast algorithm for simulating multiphase flows through periodic geometries of arbitrary shape*, SIAM J. Sci. Comput., 38 (2016), pp. B740–B772.
[24] K. M. Mayer, S. Lee, H. Liao, B. C. Rostro, A. Fuentes, P. T. Scully, C. L. Nehl, and J. H. Hafner, *A label-free immunoassay based upon localized surface plasmon resonance of gold nanorods*, ACS Nano, 2 (2008), pp. 687–692.
[25] P. Miller, *Applied Asymptotic Analysis*, American Mathematical Society, Providence, RI, 2006.
[26] L. Novotny and N. Van Hulst, *Antennas for light*, Nat. Photonics, 5 (2011), pp. 83–90.
[27] M. Rachh, A. Klöckner, and M. O'Neil, *Fast algorithms for quadrature by expansion* I: *Globally valid expansions*, J. Comput. Phys., 345 (2017), pp. 706–731.
[28] T. Sannomiya, C. Hafner, and J. Voros, *In situ sensing of single binding events by localized surface plasmon resonance*, Nano Lett., 8 (2008), pp. 3450–3455.
[29] C. Schwab and W. Wendland, *On the extraction technique in boundary integral equations*, Math. Comput., 68 (1999), pp. 91–122.
[30] D. J. Smith, *A boundary element regularized Stokeslet method applied to cilia- and flagella-driven flow*, Proc. R. Soc. Lond. A, 465 (2009), pp. 3605–3626.
[31] M. Wala and A. Klöckner, *A fast algorithm for quadrature by expansion in three dimensions*, J. Comput. Phys., 388 (2019), pp. 655–689.